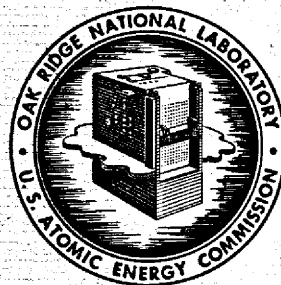


NOV 22 1967



OAK RIDGE NATIONAL LABORATORY
operated by
UNION CARBIDE CORPORATION
NUCLEAR DIVISION
for the
U.S. ATOMIC ENERGY COMMISSION



ORNL - TM - 2029

MASTER

**INVESTIGATION OF ONE CONCEPT OF A THERMAL SHIELD
FOR THE ROOM HOUSING A MOLTEN-SALT BREEDER REACTOR**

W. K. Crowley
J. R. Rose

NOTICE This document contains information of a preliminary nature and was prepared primarily for internal use at the Oak Ridge National Laboratory. It is subject to revision or correction and therefore does not represent a final report.

LEGAL NOTICE

This report was prepared as an account of Government sponsored work. Neither the United States, nor the Commission, nor any person acting on behalf of the Commission:

- A. Makes any warranty or representation, expressed or implied, with respect to the accuracy, completeness, or usefulness of the information contained in this report, or that the use of any information, apparatus, method, or process disclosed in this report may not infringe privately owned rights; or
 - B. Assumes any liabilities with respect to the use of, or for damages resulting from the use of any information, apparatus, method, or process disclosed in this report.
- As used in the above, "person acting on behalf of the Commission" includes any employee or contractor of the Commission, or employee of such contractor, to the extent that such employee or contractor of the Commission, or employee of such contractor prepares, disseminates, or provides access to, any information pursuant to his employment or contract with the Commission, or his employment with such contractor.

ORNL TM-2029

Contract No. W-7405-eng-26

General Engineering Division

INVESTIGATION OF ONE CONCEPT OF A THERMAL SHIELD
FOR THE ROOM HOUSING A MOLTEN-SALT BREEDER REACTOR

W. K. Crowley
J. R. Rose

NOVEMBER 1967

OAK RIDGE NATIONAL LABORATORY
Oak Ridge, Tennessee
operated by
UNION CARBIDE CORPORATION
for the
U. S. ATOMIC ENERGY COMMISSION

C.

10

D.

CONTENTS

	<u>Page</u>
Abstract	1
1. INTRODUCTION	1
2. SUMMARY	4
3. DEVELOPMENT OF ANALYTICAL METHODS	6
Steady-State Condition	7
Derivation of Equations	8
Calculational Procedure	15
Transient Case	17
4. PARAMETRIC STUDIES	20
Cases Studied for Steady-State Condition	20
Case Studied for Transient Condition	29
5. CONCLUSIONS	35
Appendix A. EQUATIONS NECESSARY TO CONSIDER A MULTIENERGETIC GAMMA CURRENT	41
Appendix B. EVALUATION OF THE CONVECTIVE HEAT TRANSFER COEFFICIENT	44
Appendix C. VALUES OF PHYSICAL CONSTANTS USED IN THIS STUDY . .	46
Appendix D. TSS COMPUTER PROGRAM	47
Appendix E. NOMENCLATURE	60

Q₂

Q₃

Q₄

LIST OF TABLES

<u>Table Number</u>	<u>Title</u>	<u>Page Number</u>
1	Results of Investigation of First Steady-State Case	22
2	Results of Investigation of Second Steady-State Case	23
3	Results of Investigation of Third Steady-State Case	24
4	Results of Investigation of Fourth Steady-State Case	25
5	Results of Investigation of Fifth Steady-State Case	26
6	Results of Investigation of Sixth Steady-State Case	27
7	Results of Investigation of Seventh Steady-State Case	28
8	Computer Program Used to Analyze the Proposed Reactor Room Wall for the Condition of Internal Heat Generation	31
9	Range of Parameters of Interest in Studies Made of Proposed Wall With An Incident Gamma Current of 1×10^{12} photons/cm ² ·sec	36
D.1	Typical Data for 32 Cases With One Energy Group for the TSS Computer Program	54
D.2	TSS Output Data at the Bottom of the Air Channel for One Case	58
D.3	TSS Output Data at the Top of the Air Channel for One Case	59

LIST OF FIGURES

<u>Figure Number</u>	<u>Title</u>	<u>Page Number</u>
1	Proposed Configuration of Reactor Room Wall	2
2	Proposed Configuration of Reactor Room Wall With Corresponding Terminology	6
3	Designations Given Segments of Reactor Room Wall for Study of Transient Conditions	18
4	Temperature Distribution in Proposed Reactor Room Wall With Internal Heat Generation Rate Maintained During Loss-of-Wall-Coolant Transient Period	33
5	Temperature Distribution in Proposed Reactor Room Wall With No Internal Heat Generation During the Loss-of-Wall-Coolant Transient Period	34
D.1	Assembly of Data Cards for TSS Computer Program	53

.C.

1911

The following is a list of the names of the
 persons who have been elected to the office of
 Mayor of the City of New York for the year
 1911. The names are listed in the order in
 which they were elected.

1911

.C.

INVESTIGATION OF ONE CONCEPT OF A THERMAL SHIELD FOR THE ROOM HOUSING A MOLTEN-SALT BREEDER REACTOR

Abstract

The concrete providing the biological shield for a 250-Mw(e) molten-salt breeder reactor must be protected from the gamma current within the reactor room. A configuration of a laminated shielding wall proposed for the reactor room was studied to determine (1) its ability to maintain the bulk temperature of the concrete and the maximum temperature differential at levels below the allowable maximums, (2) whether or not the conduction loss from the reactor room will be kept below a given maximum value, (3) whether air is an acceptable medium for cooling the wall, and (4) the length of time that a loss of this coolant air flow can be sustained before the bulk temperature of the concrete exceeds the maximum allowable temperature. Equations were developed to study the heat transfer and shielding properties of the proposed reactor room wall for various combinations of lamination thicknesses. The proposed configuration is acceptable for (1) an incident monoenergetic (1 Mev) gamma current of 1×10^{12} photons/cm²·sec and (2) an insulation thickness of 5 in. or more. The best results are obtained when most of the gamma-shield steel is placed on the reactor side of the cooling channel.

1. INTRODUCTION

Thermal-energy molten-salt breeder reactors (MSBR) are being studied to assess their economic and nuclear performance and to identify important design problems. One design problem identified during the study made of a conceptual 1000-Mw(e) MSBR power plant¹ was that there will be a rather intense gamma current in the room in which the molten-salt breeder reactor is housed. The concrete wall providing the biological shield around the reactor room must be protected from this intense gamma current to limit

¹P. R. Kasten, E. S. Bettis, and R. C. Robertson, "Design Studies of 1000-Mw(e) Molten-Salt Breeder Reactors," USAEC Report ORNL-3996, Oak Ridge National Laboratory, August 1966.

gamma heating in the concrete. Further, the concrete must be protected from the high ambient temperature in the reactor room. One possible method of protecting the concrete is the application of layers of gamma and thermal shielding and insulating materials on the reactor side of the concrete. A proposed configuration of the layered-type wall for the reactor room is illustrated in Fig. 1.

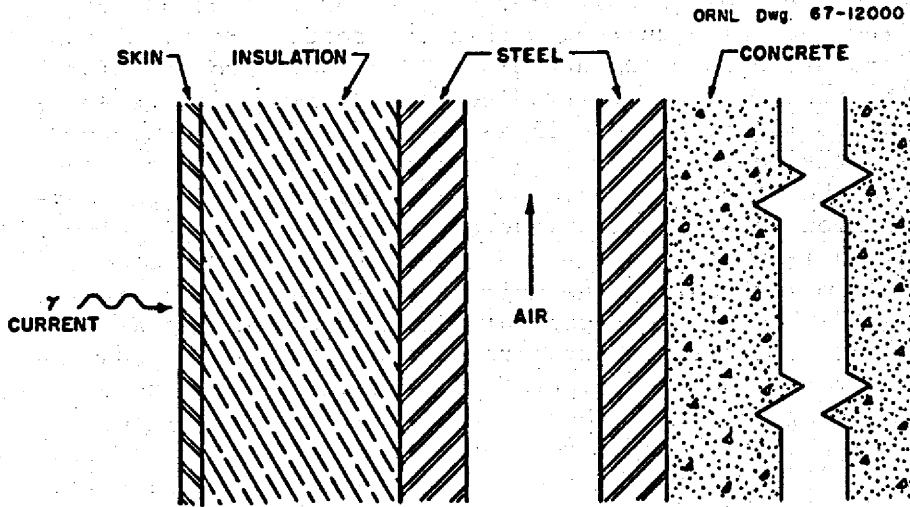


Fig. 1. Proposed Configuration of Reactor Room Wall.

The study reported here was made to investigate this proposed configuration of a reactor room wall for the modular concept¹ of a 1000-Mw(e) MSBR power plant. This modular plant would have four separate and identical 250-Mw(e) reactors with their separate salt circuits and heat-exchange loops. This preliminary investigation was made to determine whether or not the proposed configuration for the reactor room wall will

1. maintain the bulk temperature of the concrete portion of the wall at levels below 212°F,
2. maintain the temperature differential in the concrete lamination at less than 40°F (a fairly conservative value), and
3. maintain the conduction loss from a reactor room at 1 Mw or less.

This study was also performed to determine whether or not air is a suitable medium for cooling the reactor room wall and to determine the length of time over which the loss of this air flow can be tolerated before the

bulk temperature of the concrete lamination exceeds the maximum allowable temperature of 212°F.

Analysis of the proposed configuration for the wall of the reactor room was based on an investigation of the heat transfer and shielding properties of the composite wall shown in Fig. 1. Equations were developed that would allow these properties to be examined parametrically for various combinations of lamination materials and thicknesses in the wall.

2. SUMMARY

Methods were devised to parametrically analyze a composite plane wall with internal heat generation produced by the attenuation of the gamma current from the reactor room. Both steady state and transient conditions were considered. Thirty-one equations were derived and a computer program was written to examine the heat transfer and shielding properties of the proposed wall for various combinations of lamination materials and thicknesses. Incident monoenergetic (1 Mev) gamma currents of 1×10^{12} photons/cm²·sec through 3×10^{12} photons/cm²·sec were examined. A finite difference approach, with the differencing with respect to time, was used in the transient-condition analysis to obtain a first approximation of the amount of time that the proposed wall could sustain a loss of coolant air flow.

The results of these studies indicate that the proposed configuration of the laminated wall in the reactor room is acceptable for the cases considered with an incident monoenergetic (1 Mev) gamma current of 1×10^{12} photons/cm²·sec and a firebrick insulation lamination of 5 in. or more. Under these conditions, a total of approximately 4 in. of steel is sufficient for gamma shielding. The best results are obtained when the thicknesses of the mild-steel gamma shields are arranged so that the major portion of the steel is on the reactor side of the air channel. However, the proposed configuration of the laminated wall for the reactor room does not protect the concrete from excessive temperature when the incident monoenergetic gamma current is 2×10^{12} photons/cm²·sec.

With an incident monoenergetic (1 Mev) gamma current of 1×10^{12} photons/cm²·sec, the proposed laminated wall will maintain the temperature differential in the steel to within 10°F or less for all the cases studied. The differential between the temperature of the steel-concrete interface and the maximum temperature of the concrete is less than 15°F for all the cases studied. The values of both of these temperature differentials are well below a critical value.

Based on the assumption that the floor and ceiling of the reactor room have the same laminated configuration as the walls, the proposed

wall will allow the conduction loss from the reactor room to be maintained at a level below 1 Mw for an incident monoenergetic (1 Mev) gamma current of 1×10^{12} photons/cm²·sec if the thickness of the firebrick insulation lamination is 5 in. or more and if at least 4 in. of mild-steel gamma shielding is included.

With a coolant air channel width of 3 in. and an air velocity of 50 ft/sec, air is an acceptable medium for cooling the proposed reactor room wall. If the ambient temperature of the reactor room remains at approximately 1100°F and if the gamma current is maintained at 1×10^{12} photons/cm²·sec, the temperature of the concrete will remain below the critical level (212°F) for approximately one hour after a loss of the coolant air flow. If a zero incident gamma current is assumed, the "permissible" loss-of-coolant-air-flow time is greater than one hour but less than two hours.

To determine whether or not a conduction loss of 1 Mw will permit maintenance of the desired ambient temperature within the reactor room without the addition of auxiliary cooling or heating systems, an overall energy balance should be performed when sufficient information becomes available. This balance should start with the fissioning process in the reactor and extend out through the wall of the reactor room to an outside surface.

3. DEVELOPMENT OF ANALYTICAL METHODS

In the modular concept of a 1000-Mw(e) MSBR power plant,¹ the four identical but separate 250-Mw(e) molten-salt breeder reactors would be housed in four separate reactor rooms. One primary fuel-salt-to-coolant-salt heat exchanger and one blanket-salt-to-coolant-salt heat exchanger would also be housed in each reactor room along with the reactor. These items of equipment are to be located 11 ft from each other in the 52-ft-long reactor room that is 22 ft wide and 48 ft high. The reactor and the primary fuel-salt-to-coolant-salt heat exchanger are responsible for the gamma current in each of the reactor rooms. The proposed configuration of the laminations devised to protect the concrete from the gamma current in the reactor room is shown in Fig. 2 with the corresponding terminology used in the parametric studies made of the composite wall.

¹P. R. Kasten, E. S. Bettis, and R. C. Robertson, "Design Studies of 1000-Mw(e) Molten-Salt Breeder Reactors," USAEC Report ORNL-3996, Oak Ridge National Laboratory, August 1966.

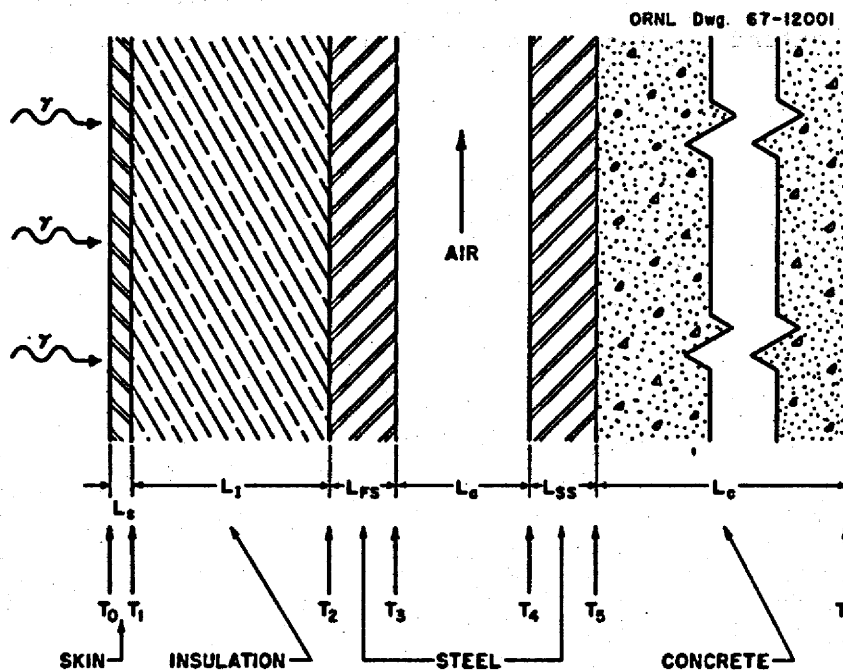


Fig. 2. Proposed Configuration of Reactor Room Wall With Corresponding Terminology.

In the direction from the interior of the reactor room out to the outer surface of the wall (left to right in Fig. 2), the layers of material comprising the wall are a stainless steel skin, firebrick insulation, a mild-steel gamma shield, an air channel, a mild-steel gamma shield, and the concrete biological shield. The thicknesses of the firebrick insulation and each of the two mild-steel gamma shields are considered to be the variable parameters in this study. The thickness of the stainless steel skin is fixed at 1/16 in., the thickness of the concrete is either 8 ft for an exterior wall or 3 ft for an interior wall, and the width of the air channel is fixed at 3 in.

The temperature of the interior surface of the reactor room wall is considered to be uniform over the surface and constant at 1100°F. The temperature of the exterior surface of the wall is considered to be uniform over the surface and constant at 50°F for the 8-ft thickness of concrete (the temperature of the earth for an exterior wall) or at 70°F for the 3-ft thickness of concrete (the ambient temperature of an adjoining room within the facility for an interior wall). The temperature of the coolant air is assumed to be 100°F at the bottom (entrance) of the air channel, and the velocity of the air is assumed to be 50 ft/sec.

The situation examined is basically one involving a composite plane wall with internal heat generation caused by the attenuation of the gamma current from the reactor room. Two conditions were considered: the steady-state condition and the transient condition. The steady-state condition was considered first and the transient condition was considered later when the problem of a loss of wall coolant was examined.

Steady-State Condition

Equations were developed to allow the heat transfer and shielding properties of the composite wall, shown in Fig. 2, to be examined parametrically for various combinations of lamination materials and thicknesses. A one-dimensional analysis was used, assuming that the temperatures of the interior and exterior surfaces of the wall were constant and uniform.

Derivation of Equations

A steady-state energy balance on a differential element of the reactor room wall can be expressed semantically as follows. The heat conducted into the element through the left face during the time $\Delta\theta$ plus the heat generated by sources in the element during the time $\Delta\theta$ equals the heat conducted out of the element through the right face during the time $\Delta\theta$. This is expressed algebraically in Eq. 1.

$$-kA_1 \left. \frac{dT}{dx} \right|_x \Delta\theta + Q(A_1 \Delta x) \Delta\theta = -kA_1 \left. \frac{dT}{dx} \right|_{x + \Delta x} \Delta\theta, \quad (1)$$

where

k = thermal conductivity, Btu/hr·ft·°F,

A_1 = unit area on wall, ft²,

T = temperature, °F,

x = distance perpendicular to surface of the wall, ft,

θ = time, hours, and

Q = volumetric gamma heating rate, Btu/hr·ft³.

Application of the mean-value theorem to dT/dx gives the expression of Eq. 2.

$$\left. \frac{dT}{dx} \right|_{x + \Delta x} = \left. \frac{dT}{dx} \right|_x + \left[\frac{d}{dx} \left(\frac{dT}{dx} \right) \right]_M \Delta x, \quad (2)$$

where M is a point between x and $x + \Delta x$. Equation 2 is substituted into Eq. 1 and $\Delta\theta$ is canceled.

$$-kA_1 \left. \frac{dT}{dx} \right|_x + Q(A_1 \Delta x) = -kA_1 \left. \frac{dT}{dx} \right|_x - kA_1 \left[\frac{d}{dx} \left(\frac{dT}{dx} \right) \right]_M \Delta x. \quad (3)$$

The common term $-kA_1 \left. \frac{dT}{dx} \right|_x$ is canceled, and it is noted that $\frac{d}{dx} \left(\frac{dT}{dx} \right) = d^2T/dx^2$. The resulting expression is given in Eq. 4.

$$QA_1 \Delta x = -kA_1 \left. \frac{d^2T}{dx^2} \right|_M \Delta x. \quad (4)$$

Dividing Eq. 4 by $A_1 \Delta x$ and allowing Δx to approach zero as a limit so that a value at M becomes a value at x , the volumetric gamma heating rate,

$$Q = -k \frac{d^2T}{dx^2}. \quad (5)$$

Equation 5 is integrated twice, and if $Q \neq Q(x)$,

$$T(x) = -\frac{Q}{2k} x^2 + C_1 x + C_2 . \quad (6)$$

The applicable boundary conditions for any particular lamination in the wall are $T = T_0$ at $x = 0$ and $T = T_L$ at $x = L$, where T_0 = the temperature of the lamination interface at zero location designated in Fig. 2 and L = the thickness of the material in a lamination in feet. These conditions are applied to Eq. 6.

$$T(x) = T_0 + \frac{x}{L}(T_L - T_0) + \frac{Q}{2k}(Lx - x^2) . \quad (7)$$

The internal heat generation encountered in this study is caused by a deposition of energy in the form of heat when the gamma rays are attenuated by the materials in the wall of the room. Because of this attenuation of the gamma rays, the volumetric gamma heating rate, Q , is a function of the distance perpendicular to the surface of the wall, x . The equations derived in this study are based on the assumption that the incident gamma current is monoenergetic, but appropriate equations for a multi-energetic gamma current are given in Appendix A. For a mono-energetic gamma current where buildup and exponential attenuation are considered, the equation for $Q(x)$ becomes

$$Q(x) = Q_0 \left[A e^{\alpha \mu x} + (1 - A) e^{-\beta \mu x} \right] e^{-\mu x} , \quad (8)$$

where

A , α , and β = dimensionless constants used in the Taylor buildup equation

and μ = the total gamma attenuation coefficient, ft^{-1} .

When

$$Q_0 = E \Phi_0 \mu_E ,$$

$$Q(x) = Q_0 \left[A e^{\mu x (\alpha - 1)} + (1 - A) e^{-\mu x (\beta + 1)} \right] , \quad (9)$$

where

Q_0 = the volumetric gamma heating rate at the surface on the reactor side of the stainless steel skin, $\text{Btu/hr} \cdot \text{ft}^3$,

E = energy of the incident gamma current, Mev,

Φ_0 = incident gamma current, photons/ $\text{cm}^2 \cdot \text{sec}$, and

μ_E = gamma energy attenuation coefficient, ft^{-1} .

Substituting Eq. 9 into Eq. 5,

$$\frac{d^2 T}{dx^2} + \frac{Q_0}{k} \left[A e^{\mu x(\alpha - 1)} + (1 - A) e^{-\mu x(\beta + 1)} \right] = 0. \quad (10)$$

Equation 10 is integrated twice to yield

$$T(x) = - \frac{Q_0}{k\mu^2} \left[\frac{A}{(\alpha - 1)^2} e^{\mu x(\alpha - 1)} + \frac{(1 - A)}{\mu^2 (\beta + 1)^2} e^{-\mu x(\beta + 1)} \right] + C_3 x + C_4 = 0. \quad (11)$$

The previously stated boundary conditions are still applicable, and the result of applying these conditions to Eq. 11 is that

$$T(x) = T_0 + \frac{x}{L}(T_L - T_0) + \frac{Q_0}{k\mu^2} \left\{ \left[\frac{A}{(\alpha - 1)^2} (1 - e^{\mu x(\alpha - 1)}) + \frac{1 - A}{(\beta + 1)^2} (1 - e^{-\mu x(\beta + 1)}) \right] - \frac{x}{L} \left[\frac{A}{(\alpha - 1)^2} (1 - e^{\mu L(\alpha - 1)}) + \frac{1 - A}{(\beta + 1)^2} (1 - e^{-\mu L(\beta + 1)}) \right] \right\} \quad (12)$$

The temperature distribution in any particular lamination of the wall is given by Eq. 12 when the appropriate constants for that lamination are used. Equation 12 is used primarily to determine the maximum temperature in the concrete and to determine the location of this maximum temperature. To locate the position of the maximum temperature in the concrete, Eq. 12 is differentiated with respect to x , the resulting derivative (dT/dx) is set equal to zero, and the equation is solved for x . The value of x obtained gives the distance from the concrete-steel interface to the position of the maximum temperature in the concrete.

$$\frac{dT}{dx} = \frac{1}{L}(T_L - T_0) + \frac{Q_0}{k\mu^2} \left\{ \left[\frac{A\mu}{(\alpha - 1)} (-e^{\mu x(\alpha - 1)}) + \frac{\mu(1 - A)}{\beta + 1} (+ e^{-\mu x(\beta + 1)}) \right] - \frac{1}{L} \left[\frac{A}{(\alpha - 1)^2} (1 - e^{\mu L(\alpha - 1)}) + \frac{1 - A}{(\beta + 1)^2} (1 - e^{-\mu L(\beta + 1)}) \right] \right\} = 0. \quad (13)$$

Equation 13 is a transcendental equation in x , and as such, it must be solved by using a trial-and-error technique. There are only two terms in Eq. 13 that contain x , and these terms are rearranged to put Eq. 13 in a form more easily solved by trial and error.

$$\begin{aligned} & \frac{Q_0(1-A)}{\mu k(\beta+1)} e^{-\mu x(\beta+1)} - \frac{Q_0 A}{\mu k(\alpha-1)} e^{\mu x(\alpha-1)} \\ &= \frac{1}{L}(T_0 - T_L) + \frac{1}{L} \left(\frac{Q_0}{k\mu^2} \right) \left[\frac{A}{(\alpha-1)^2} (1 - e^{\mu L(\alpha-1)}) \right. \\ & \quad \left. + \frac{1-A}{(\beta+1)^2} (1 - e^{-\mu L(\alpha-1)}) \right] . \end{aligned} \quad (14)$$

All of the coefficients on the left side of Eq. 14 are known, and all of the terms on the right side are known. Therefore, Eq. 14 may be written in the form

$$K_1 e^{-a_1 x} + K_2 e^{-a_2 x} = K_3 , \quad (15)$$

where the K's and a's are calculable numbers. When Eq. 14 is solved for x, this value of x is called $x_{T \max}$. The value $x = x_{T \max}$ is substituted into Eq. 12 to obtain the maximum temperature of the concrete.

To determine the magnitude of the conduction loss, q^* , from the reactor room, equations were written to give the temperature drops across each separate lamination in the wall. These equations are simple conduction and convection equations in which all of the heat generated in a particular lamination is assumed to be conducted through a length equal to two-thirds of the thickness of the particular lamination. The total amount of gamma heat, q_T , deposited per unit area in a direction normal to the face of the wall is found for any particular lamination by integrating Eq. 9 over the length, L, of the particular lamination.

$$q_T = \int_0^L Q_0 \left[A e^{\mu x(\alpha-1)} + (1-A) e^{-\mu x(\beta+1)} \right] dx \quad (16)$$

$$= \frac{Q_0}{\mu} \left[\frac{A}{(\alpha-1)} (e^{\mu L(\alpha-1)} - 1) - \frac{1-A}{\beta+1} (e^{-\mu L(\beta+1)} - 1) \right] , \quad (17)$$

where Q_0 is the incident volumetric gamma heating rate.

There are two possible ways to evaluate the incident volumetric gamma heating rate at some particular material interface, which shall be referred to as the "j-th" interface. The first way is to calculate the gamma current, $\Phi_{o(j)}$, at each interface. To obtain $Q_{o(j)}$, this calculated value of $\Phi_{o(j)}$ is substituted into the equation

$$Q_{o(j)} = E \Phi_{o(j)} \mu_E .$$

The second method of evaluating the incident volumetric gamma heating rate involves subtracting the total amount of gamma heat deposited per unit area in the j -th lamination, q_j , from the gamma energy current per unit area incident upon the j -th lamination, $q_{o(j)}$, to approximate the gamma energy current per unit area incident upon the face of the following lamination $q_{o(j+1)}$.

$$q_{o(j+1)} = q_{o(j)} - q_j \quad (18)$$

The volumetric gamma heating rate incident upon a particular lamination, $Q_{o(j)}$, and the gamma energy current per unit area incident upon the j -th lamination, $q_{o(j)}$, are related by the following equation.

$$q_{o(j)} = Q_{o(j)} / \mu_E(j) \quad (18a)$$

Therefore,

$$Q_{o(j+1)} = q_{o(j+1)} \mu_E(j+1) \quad (18b)$$

These two methods are in fairly good agreement, and since the values for the various material constants were not well fixed at this point in the design for the reactor room wall, the second method of evaluating the incident volumetric gamma heating rate was used in this study. The second method is simpler to use and easier to calculate.

The equations for the steady-state temperature drops across each of the material laminations on the reactor side of the air channel are given below and the temperature points are as illustrated in Fig. 2.

$$T_0 - T_1 = \frac{(q^* + \frac{2}{3}q_s)L_s}{k_s} \quad (19)$$

where

q^* = heat conduction rate out of the reactor room, Btu/hr·ft²,

q_s = gamma heat deposition rate in the stainless steel outer skin, Btu/hr·ft²,

L_s = thickness of the stainless steel skin, ft, and

k_s = thermal conductivity of the stainless steel skin, Btu/hr·ft·°F.

$$T_1 - T_2 = \frac{(q^* + q_s + \frac{2}{3}q_I)L_I}{k_I}, \quad (20)$$

where the subscript I refers to the insulation lamination shown in Fig. 2.

$$T_2 - T_3 = \frac{(q^* + q_s + q_I + \frac{2}{3}q_{FS})L_{FS}}{k_{FS}}, \quad (21)$$

where the subscript FS refers to the first mild-steel gamma shield (on the reactor side of the air channel).

$$T_3 - T_a = \frac{q^* + q_s + q_I + q_{FS}}{h}, \quad (22)$$

where

T_a = temperature of the air in the channel, °F, and

h = convective heat transfer coefficient, Btu/hr·ft²·°F.

The average convective heat transfer coefficient across the walls of the air channel is evaluated in Appendix B, and the value of 5 was determined for a mean temperature of from 130 to 150°F. It was assumed that the gamma heating in the air channel is negligible. Equations 19, 20, 21, and 22 were added and the resulting equation was solved for q^* . The heat conduction rate out of the reactor room to the air channel,

$$q^* = \frac{(T_o - T_a) - q_s \left[\left(\frac{2}{3} \right) \frac{L_s}{k_s} + \frac{L_I}{k_I} + \frac{L_{FS}}{k_{FS}} + \frac{1}{h} \right] - q_I \left[\left(\frac{2}{3} \right) \frac{L_I}{k_I} + \frac{L_{FS}}{k_{FS}} + \frac{1}{h} \right] - q_{FS} \left[\left(\frac{2}{3} \right) \frac{L_{FS}}{k_{FS}} + \frac{1}{h} \right]}{\left(\frac{L_s}{k_s} + \frac{L_I}{k_I} + \frac{L_{FS}}{k_{FS}} + \frac{1}{h} \right)}. \quad (23)$$

On the concrete side of the air channel, the value of primary interest is the maximum temperature of the concrete, T_{max} . This temperature may be determined by using Eqs. 12 and 14, but the temperature of the steel-concrete interface, T_5 , must be known before these equations can be used. The simple conduction and convection equations for the laminated wall on the concrete side of the air channel are given below.

$$T_4 - T_a = \frac{q_{SS} + q'_c + q_R}{h}, \quad (24)$$

where

q_{SS} = gamma heat deposition rate in the second mild-steel gamma shield, Btu/hr·ft²,

q'_c = rate at which the gamma heat generated in the concrete is conducted back toward the air channel, Btu/hr·ft², and

q_R = radiant heat transfer rate between the walls of the air channel, Btu/hr·ft²,

$$q_R = \frac{\sigma}{\frac{2}{\epsilon} - 1} (T_3^4 - T_4^4)$$

where

σ = Stefan-Boltzmann constant

$$= 0.1714 \times 10^{-8}$$

ϵ = surface emissivity of air channel walls, assumed to the same for both surfaces.

$$T_6 - T_4 = \frac{(q'_c + \frac{2}{3}q_{SS})L_{SS}}{k_{SS}} \quad (26)$$

In this study, there is a point in the concrete at which the temperature of the concrete is a maximum. All of the gamma heat generated on the air channel side of that point will be conducted toward the air channel; that is, in the direction of decreasing temperature. This amount of heat, q'_c , may be calculated by evaluating dT/dx in the concrete at $x = 0$, using Eq. 13.

$$\left. \frac{dT}{dx} \right|_{x=0} = \frac{1}{L_c}(T_6 - T_6) + \frac{Q_{o(c)}}{k_c \mu^2} \left\{ \left[-\frac{A\mu}{(\alpha - 1)} + \frac{\mu(1 - A)}{\beta + 1} \right] - \frac{1}{L_c} \left[\frac{A}{(\alpha - 1)^2} \left(1 - e^{-\mu L_c(\alpha - 1)} \right) + \frac{1 - A}{(\beta + 1)^2} \left(1 - e^{-\mu L_c(\beta + 1)} \right) \right] \right\}, \quad (27)$$

recognizing that

$$q'_c = k_c \left. \frac{dT}{dx} \right|_{x=0}, \quad (28)$$

where the subscript c denotes concrete. The right side of Eq. 28 is positive rather than negative because Eq. 27 makes positive conduction in the direction from the air channel toward the concrete, but q'_c is

to be made positive in the direction from the concrete toward the air channel. Equations 24, 25, 26, 27, and 28 were combined to yield one equation in which the only unknown is T_4 . The value for T_3 can be calculated from the equations for the reactor side of the air channel.

$$\left(\frac{\sigma}{\epsilon} - 1\right) T_4^4 + T_4 \left(h + \frac{1}{\frac{L_{SS}}{k_{SS}} + \frac{L_c}{k_c}} \right) = \left(\frac{\sigma}{\epsilon} - 1\right) T_3^4 + hT_a + q_{SS} + \frac{T_E + \frac{L_c Q_o(c)}{k_c \mu^2} B' - \frac{2L_{SS} q_{SS}}{3k_{SS}}}{\frac{L_{SS}}{k_{SS}} + \frac{L_c}{k_c}}, \quad (29)$$

where

$$B' = \left(\frac{\mu(1-A)}{\beta+1} - \frac{\mu A}{(\alpha-1)} \right) - \frac{1}{L_c} \left[\frac{A}{(\alpha-1)^2} \left(1 - e^{-\mu L_c (\alpha-1)} \right) + \frac{1-A}{(\beta+1)^2} \left(1 - e^{-\mu L_c (\beta+1)} \right) \right]. \quad (29a)$$

The constants in Eq. 29a that have no identifying subscripts are understood to be for concrete. Equation 29 is also a transcendental equation. Therefore, a trial-and-error method must be used to solve for T_4 . Once T_4 and q'_c are known, T_5 can be calculated by using Eq. 25.

Calculational Procedure

Since the calculation of certain of the desired quantities requires that the value of other desired quantities be known, there is a certain order in which the problem must be worked. For a particular case, the thickness of each of the laminations in the wall is selected, and the inside (reactor room) and outside (earth or internal) wall temperatures are specified. The incident gamma current and the temperature of the coolant air are also specified. The constants for the various equations are selected, and those used are given in Appendix C.

With the proper constants for each different lamination, Eq. 17 is first used to calculate the gamma heat depositions in each of the separate laminations (q_s , q_I , q_{FS} , q_{SS} , and q_c). Equation 23 is then used to calculate the conduction loss from the reactor room q^* . The temperature drops and the interface temperatures on the reactor side of the air channel are calculated by using Eqs. 19, 20, 21, and 22. Equation 29 is used to calculate the value of T_4 , and then the value of q_R is calculated by using Eq. 25. Then q'_c is calculated by using Eq. 24, and the value of T_5 is calculated by using Eq. 26. Once the value of T_5 is known, $x_{T \max}$ is obtained by using Eq. 14, and the maximum temperature of the concrete is calculated by evaluating Eq. 12 at $x = x_{T \max}$.

At this point, it is possible to calculate the vertical temperature gradient ($^{\circ}\text{F}/\text{ft}$) in the coolant air. This temperature gradient,

$$\Delta T = \frac{q_s + q_I + q_{FS} + q_{SS} + q^* + q_R + q'_c}{3600 U_a \rho_a L_{ch} C_{p_a}}, \quad (30)$$

where

U_a = bulk velocity of coolant air, ft/sec,

ρ_a = density of air, lb/ft³,

L_{ch} = width of air channel (distance between steel laminations), ft,

C_{p_a} = specific heat of air at constant pressure, Btu/lb $\cdot^{\circ}\text{F}$.

The temperature of the air at the top of the channel,

$$T'_a = T_a + \Delta T(H), \quad (31)$$

where H = the vertical length of the air channel in feet.

The entire calculational procedure can now be repeated using the new air temperature at the top of the air channel, T'_a . This calculation of the temperature of the air at the top of the channel is necessary because a higher T_a causes the maximum temperature of the concrete to be higher, and the magnitude of this maximum temperature is one of the constraints in this study.

A program was developed for the CDC 1604-A computer to solve Eqs. 8 through 31 for the steady-state condition. The TSS (Thermal Shield Study)

computer program is described in Appendix D. The program performs the calculations in the order described above, and it will handle up to five material laminations (excluding the air channel) in the proposed reactor room wall and up to eight energy groups for the incident gamma current.

Transient Case

The problem of the loss of coolant for the reactor room wall is basically a transient heat conduction problem with internal heat generation. If the flow of coolant air through the channel in the wall is lost for an appreciable length of time, the temperature in the concrete and/or the steel laminations may become excessive. To investigate this situation with the goal of obtaining a first approximation of the amount of time that such a loss of air flow could be sustained safely, a finite difference approach was taken. The differencing is with respect to time and the superscript n in the following equations denotes values after the n -th time interval.

The proposed configuration of the reactor room wall was broken into segments of given lengths with nodal points located at the center of each segment, as shown in Fig. 3. Each segment in the concrete region of the wall was assumed to be 1 ft thick, each segment in the mild-steel gamma shields and in the firebrick insulation was assumed to be 1 in. thick, the entire stainless steel skin was treated as a single segment 1/16 in. thick, and the air channel was treated as a single segment 3 in. thick.

The energy balance for a particular segment can be expressed semantically as follows. The heat conducted into a segment during the time $\Delta\theta$ plus the heat generated in the segment during the time $\Delta\theta$ equals the heat stored in the segment during the time $\Delta\theta$ plus the heat conducted out of the segment during the time $\Delta\theta$. The corresponding algebraic equation for a typical segment of the composite wall is given below with Segment 4 selected for illustrative purposes.

$$\frac{k A}{L_c} (T_5^n - T_4^n) + q_4 c A = \frac{\rho_c A L_c c_p}{\Delta\theta} (T_4^{n+1} - T_4^n) + \frac{k A}{L_c} (T_4^n - T_3^n). \quad (32)$$

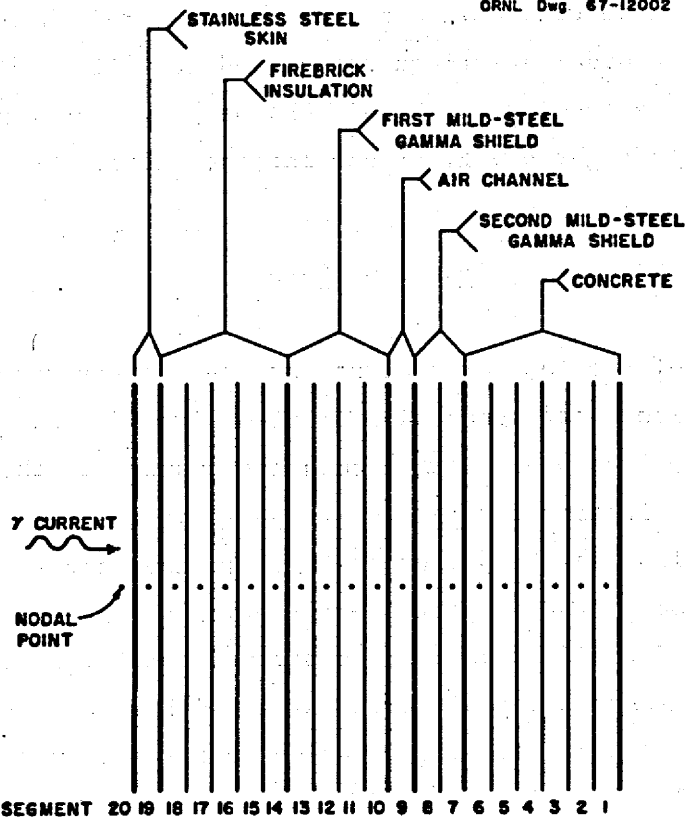


Fig. 3. Designations Given Segments of Reactor Room Wall for Study of Transient Conditions.

Rearranging Eq. 32,

$$T_4^{n+1} = T_4^n + \frac{k_c \Delta \theta}{\rho_c L_c^2 C_p c} (T_5^n - 2T_4^n + T_3^n) + \frac{q_4 \Delta \theta}{\rho_c L_c C_p c}. \quad (33)$$

A characteristic equation at an interface between two different materials is given in Eq. 34.

$$T_7^{n+1} = T_7^n + \frac{k_s \Delta \theta}{\rho_s L_s^2 C_p s} (T_8^n - T_7^n) + \frac{\bar{k}_{s-c} \Delta \theta}{\rho_s L_s L_c C_p s} (T_8^n - T_7^n) + \frac{q_7 \Delta \theta}{\rho_s L_s C_p s}, \quad (34)$$

where the subscript s denotes the stainless steel skin, the subscript c denotes the concrete, and \bar{k}_{s-c} is an equivalent conductivity given by Eq. 35.

$$\bar{k}_{a-b} = \frac{k_a k_b (L_a + L_b)}{k_a L_b + k_b L_a}, \quad (35)$$

where the subscripts a and b refer to any two adjacent materials.

Eighteen equations similar to those just given were derived to carry the analysis across the entire reactor room wall, and a simple computer program was written to perform the calculations required for one specific transient condition.

4. PARAMETRIC STUDIES

The parametric studies of the proposed configuration of a laminated wall for the reactor room, shown in Fig. 2, to protect the concrete biological shield from the gamma current within the room were made for two conditions: the steady-state condition and the transient condition.

Parametric studies of the material laminations for the steady-state condition were made to determine whether or not

1. the bulk temperature of the concrete portion of the wall could be maintained at levels below 212°F ,
2. the temperature differential in the concrete could be maintained at less than 40°F , and
3. the conduction loss for a reactor room could be maintained at 1 Mw or less.

A transient condition was investigated to determine the length of time over which the loss of coolant air flow could be tolerated before the temperature of the concrete would exceed the maximum allowable temperature of 212°F .

Cases Studied for Steady-State Condition

For the parametric analysis of the composite plane wall with internal heat generation for steady-state conditions, the air channel was not considered as a material lamination but rather as having a fixed width of 3 in. between the first and second mild-steel gamma shields. The temperature of the incoming cooling air at the bottom of the air channel was assumed to be 100°F , and the velocity of the air was set at 50 ft/sec. The thickness of the stainless steel skin on the reactor side or interior surface of the wall was fixed at $1/16$ in., and the temperature of the interior surface of the reactor room wall was considered to be uniform over the surface and constant at 1100°F . Equations 8 through 31 derived in Chapter 3 were used with the TSS computer program described in Appendix D to examine the steady-state effects of changing the

1. thickness of the firebrick insulation,
2. total amount of mild steel used for the gamma shields,
3. ratio of the amount of steel on the reactor side of the air channel to the amount of steel on the concrete side of the air channel,
4. thickness and outside temperature of the concrete wall, and the
5. magnitude of the incident monoenergetic (1 Mev) gamma current.

Sixty-four separate cases were analyzed for the steady-state condition to determine the effects of changing those parameters of interest. Data illustrative of the typical effects of varying the parameters were selected from the results of these analyses and are compiled in Tables 1 through 7. The effects of changing the parameters are given for incident gamma currents of 1×10^{12} and 2×10^{12} photons/cm²·sec in all of these tables, and the conditions at the bottom (entrance) and top (exit) of the air channel are given for both magnitudes of incident gamma current.

For cases with an incident gamma current of 1×10^{12} photons/cm²·sec, the maximum temperature of the concrete increases approximately 50°F from the bottom of the air channel to the top. For cases with an incident gamma current of 2×10^{12} photons/cm²·sec and no conduction back to the reactor room, the maximum temperature of the concrete increases approximately 80°F from the bottom to the top of the air channel. For a given gamma current and insulation thickness, the conduction loss changes very little (about 0.04 Mw) between the bottom and the top of the air channel.

The largest value for the maximum temperature of the concrete at the top of the air channel in those cases with an incident gamma current of 1×10^{12} photons/cm²·sec and an insulation thickness of 5 in. or more is approximately 200°F. On the other hand, the smallest value for the maximum temperature of the concrete at the top of the air channel in those cases with an incident gamma current of 2×10^{12} photons/cm²·sec and an insulation thickness of 5 in. or more is greater than 250°F.

Table 1. Results of Investigation of First Steady-State Case

Case Conditions Studied				
	$T_o = 1100^{\circ}\text{F}$	$L_c = 8 \text{ ft}$	$T_s = 50^{\circ}\text{F}$	
	$L_g = 1/16 \text{ in.}$	$L_I = 5 \text{ in.}$	$L_{FS} = 4 \text{ in.}$	$L_{SS} = 2 \text{ in.}$
	$\phi_o = 1 \times 10^{12} \text{ photons/cm}^2 \cdot \text{sec}$		$\phi_o = 2 \times 10^{12} \text{ photons/cm}^2 \cdot \text{sec}$	
	Bottom of Channel	Top of Channel	Bottom of Channel	Top of Channel
$q_g, \text{ Btu/hr} \cdot \text{ft}^2$	16.57	16.57	33.14	33.14
$q_I, \text{ Btu/hr} \cdot \text{ft}^2$	75.47	75.47	151.0	151.0
$q_{FS}, \text{ Btu/hr} \cdot \text{ft}^2$	370.6	370.6	741.2	741.2
$q_{SS}, \text{ Btu/hr} \cdot \text{ft}^2$	11.69	11.69	23.38	23.38
$q_c, \text{ Btu/hr} \cdot \text{ft}^2$	33.65	33.65	67.30	67.30
$q_c', \text{ Btu/hr} \cdot \text{ft}^2$	25.84	22.04	55.31	48.99
$q_R, \text{ Btu/hr} \cdot \text{ft}^2$	110.6	131.2	198.9	253.9
MWL, Mw	0.5812	0.5382	0.3520	0.2838
$T_1, ^{\circ}\text{F}$	1099.9	1099.9	1099.9	1099.9
$T_2, ^{\circ}\text{F}$	247.9	297.1	324.6	402.7
$T_3, ^{\circ}\text{F}$	240.5	289.9	314.1	392.5
$T_4, ^{\circ}\text{F}$	100.0	153.0	100.0	184.0
$T_5, ^{\circ}\text{F}$	129.6	186.0	155.5	249.3
$T_6, ^{\circ}\text{F}$	129.8	186.2	156.0	249.7
$T_o - T_1, ^{\circ}\text{F}$	0.1018	0.0946	0.0679	0.0565
$T_1 - T_2, ^{\circ}\text{F}$	852.0	802.8	775.3	697.3
$T_2 - T_3, ^{\circ}\text{F}$	7.412	7.185	10.55	10.19
$T_3 - T_4, ^{\circ}\text{F}$	140.5	136.9	214.1	208.5
$T_4 - T_5, ^{\circ}\text{F}$	29.63	32.98	55.52	65.25
$T_5 - T_6, ^{\circ}\text{F}$	0.216	0.1916	0.4554	0.4148
$T_{\text{max}}, ^{\circ}\text{F}$	140.5	193.6	181.3	268.5
$x_{T \text{ max}}, \text{ ft}$	0.5422	0.4083	0.6343	0.4887
$\Delta T/H, ^{\circ}\text{F/ft}$	1.104	1.103	1.751	1.777

Table 2. Results of Investigation of Second Steady-State Case

	Case Conditions Studied			
	$T_0 = 1100^\circ\text{F}$		$T_8 = 70^\circ\text{F}$	
	$L_s = 1/16$ in.	$L_c = 3$ ft $L_I = 5$ in.	$L_{FS} = 4$ in.	$L_{SS} = 2$ in.
	$\phi_0 = 1 \times 10^{12}$ photons/cm ² ·sec		$\phi_0 = 2 \times 10^{12}$ photons/cm ² ·sec	
	Bottom of Channel	Top of Channel	Bottom of Channel	Top of Channel
q_s , Btu/hr·ft ²	16.57	16.57	33.14	33.14
q_I , Btu/hr·ft ²	75.47	75.47	151.0	151.0
q_{FS} , Btu/hr·ft ²	370.6	370.6	741.2	741.2
q_{SS} , Btu/hr·ft ²	11.69	11.69	23.38	23.38
q_c , Btu/hr·ft ²	33.65	33.65	67.30	67.30
q_c' , Btu/hr·ft ²	18.33	8.446	42.64	26.19
q_R , Btu/hr·ft ²	111.6	133.3	200.8	258.2
MWL, Mw	0.5812	0.5385	0.3520	0.2845
T_1 , °F	1099.9	1099.9	1099.9	1099.9
T_2 , °F	247.9	296.7	324.6	402.1
T_3 , °F	240.5	289.5	314.1	391.9
T_a , °F	100.0	152.6	100.0	183.4
T_4 , °F	128.3	183.3	153.4	244.9
T_5 , °F	128.5	183.4	153.7	245.2
$T_0 - T_1$, °F	0.1018	0.0947	0.0679	0.0566
$T_1 - T_2$, °F	852.0	803.2	775.3	697.9
$T_2 - T_3$, °F	7.412	7.187	10.55	10.19
$T_3 - T_a$, °F	140.5	136.9	214.1	208.5
$T_4 - T_a$, °F	28.32	30.68	53.36	60.55
$T_5 - T_4$, °F	0.1678	0.1043	0.3740	0.2683
T_{max} , °F	133.4	184.4	167.4	250.0
$x_{T_{max}}$, ft	0.3124	0.1276	0.3878	0.2061
$\Delta T/H$, °F/ft	1.096	1.088	1.737	1.754

Table 3. Results of Investigation of Third Steady-State Case

	Case Conditions Studied			
	$T_0 = 1100^\circ\text{F}$		$T_6 = 50^\circ\text{F}$	
	$L_s = 1/16$ in.	$L_c = 8$ ft	$L_{FS} = 2$ in.	$L_{SS} = 4$ in.
	$\phi_0 = 1 \times 10^{12}$ photons/cm ² ·sec		$\phi_0 = 2 \times 10^{12}$ photons/cm ² ·sec	
	Bottom of Channel	Top of Channel	Bottom of Channel	Top of Channel
q_g , Btu/hr·ft ²	16.57	16.57	33.14	33.14
q_I , Btu/hr·ft ²	75.47	75.47	151.0	151.0
q_{FS} , Btu/hr·ft ²	299.6	299.6	599.2	599.2
q_{SS} , Btu/hr·ft ²	82.69	82.69	165.4	165.4
q_c , Btu/hr·ft ²	33.65	33.65	67.30	67.30
q_c' , Btu/hr·ft ²	25.15	21.50	54.08	48.21
q_R , Btu/hr·ft ²	87.31	102.6	141.5	177.6
MWL, Mw	0.5960	0.5538	0.3799	0.3139
T_1 , °F	1099.9	1099.9	1099.9	1099.9
T_2 , °F	230.9	279.2	292.7	368.2
T_3 , °F	227.5	275.9	288.0	363.6
T_4 , °F	100.0	151.9	100.0	181.1
T_4' , °F	139.0	193.3	172.2	259.3
T_5 , °F	140.1	194.2	174.3	261.4
$T_0 - T_1$, °F	0.1043	0.0972	0.0276	0.0616
$T_1 - T_2$, °F	869.0	820.7	807.2	731.7
$T_2 - T_3$, °F	3.452	3.341	4.754	4.580
$T_3 - T_4$, °F	127.5	124.0	188.0	182.5
$T_4 - T_4'$, °F	39.03	41.35	72.19	78.24
$T_5 - T_4$, °F	1.028	0.9814	2.105	2.030
T_{max} , °F	150.1	201.2	198.2	279.5
x_T max, ft	0.5139	0.3927	0.6004	0.4745
$\Delta T/H$, °F/ft	1.081	1.074	1.689	1.694

Table 4. Results of Investigation of Fourth Steady-State Case

Case Conditions Studied				
	$T_o = 1100^{\circ}\text{F}$	$L_c = 3 \text{ ft}$	$T_6 = 70^{\circ}\text{F}$	
	$L_s = 1/16 \text{ in.}$	$L_I = 5 \text{ in.}$	$L_{FS} = 2 \text{ in.}$	$L_{SS} = 4 \text{ in.}$
	$\phi_o = 1 \times 10^{12} \text{ photons/cm}^2 \cdot \text{sec}$		$\phi_o = 2 \times 10^{12} \text{ photons/cm}^2 \cdot \text{sec}$	
	Bottom of Channel	Top of Channel	Bottom of Channel	Top of Channel
$q_g, \text{ Btu/hr} \cdot \text{ft}^2$	16.57	16.57	33.14	33.14
$q_I, \text{ Btu/hr} \cdot \text{ft}^2$	75.47	75.47	151.0	151.0
$q_{FS}, \text{ Btu/hr} \cdot \text{ft}^2$	299.6	299.6	599.2	599.2
$q_{SS}, \text{ Btu/hr} \cdot \text{ft}^2$	82.69	82.69	165.4	165.4
$q_c, \text{ Btu/hr} \cdot \text{ft}^2$	33.65	33.65	67.30	67.30
$q_c', \text{ Btu/hr} \cdot \text{ft}^2$	16.53	7.048	39.42	24.17
$q_p, \text{ Btu/hr} \cdot \text{ft}^2$	88.49	104.9	143.8	182.4
MWL, Mw	0.5960	0.5543	0.3799	0.3146
$T_1, ^{\circ}\text{F}$	1099.9	1099.9	1099.9	1099.9
$T_2, ^{\circ}\text{F}$	230.9	278.8	292.7	367.5
$T_3, ^{\circ}\text{F}$	227.5	275.5	288.0	362.9
$T_a, ^{\circ}\text{F}$	100.0	151.4	100.0	180.3
$T_4, ^{\circ}\text{F}$	137.5	190.4	169.7	254.7
$T_5, ^{\circ}\text{F}$	138.5	191.2	171.6	256.4
$T_o - T_1, ^{\circ}\text{F}$	0.1043	0.0973	0.0726	0.0617
$T_1 - T_2, ^{\circ}\text{F}$	869.0	821.1	807.2	732.4
$T_2 - T_3, ^{\circ}\text{F}$	3.452	3.342	4.754	4.581
$T_3 - T_a, ^{\circ}\text{F}$	127.5	124.0	188.0	182.6
$T_4 - T_a, ^{\circ}\text{F}$	37.54	38.93	69.71	74.40
$T_5 - T_4, ^{\circ}\text{F}$	0.9178	0.7963	1.917	1.722
$T_{\text{max}}, ^{\circ}\text{F}$	142.4	192.8	183.1	260.5
$x_{T \text{ max}}, \text{ ft}$	0.2724	0.1052	0.3454	0.1881
$\Delta T/H, ^{\circ}\text{F/ft}$	1.072	1.058	1.673	1.669

Table 5. Results of Investigation of Fifth Steady-State Case

Case Conditions Studied				
	$T_0 = 1100^\circ\text{F}$	$L_c = 8 \text{ ft}$	$T_6 = 50^\circ\text{F}$	
	$L_g = 1/16 \text{ in.}$	$L_I = 5 \text{ in.}$	$L_{FS} = 2 \text{ in.}$	$L_{SS} = 2 \text{ in.}$
	$\phi_0 = 1 \times 10^{12} \text{ photons/cm}^2 \cdot \text{sec}$		$\phi_0 = 2 \times 10^{12} \text{ photons/cm}^2 \cdot \text{sec}$	
	Bottom of Channel	Top of Channel	Bottom of Channel	Top of Channel
$q_g, \text{ Btu/hr} \cdot \text{ft}^2$	16.57	16.57	33.14	33.14
$q_I, \text{ Btu/hr} \cdot \text{ft}^2$	75.47	75.47	151.0	151.0
$q_{FS}, \text{ Btu/hr} \cdot \text{ft}^2$	299.6	299.6	599.2	599.2
$q_{SS}, \text{ Btu/hr} \cdot \text{ft}^2$	71.15	71.15	142.3	142.3
$q_c, \text{ Btu/hr} \cdot \text{ft}^2$	45.19	45.19	90.38	90.38
$q_c', \text{ Btu/hr} \cdot \text{ft}^2$	35.90	32.24	75.58	69.71
$q_R, \text{ Btu/hr} \cdot \text{ft}^2$	87.42	102.7	141.7	177.9
MWL, Mw	0.5960	0.5538	0.3799	0.3141
$T_1, ^\circ\text{F}$	1099.9	1099.9	1099.9	1099.9
$T_2, ^\circ\text{F}$	230.9	279.2	292.7	368.1
$T_3, ^\circ\text{F}$	227.5	275.9	288.0	363.6
$T_a, ^\circ\text{F}$	100.0	151.9	100.0	181.0
$T_4, ^\circ\text{F}$	138.9	193.1	171.9	259.0
$T_5, ^\circ\text{F}$	139.4	193.6	173.0	260.1
$T_0 - T_1, ^\circ\text{F}$	0.1043	0.0972	0.0726	0.0616
$T_1 - T_2, ^\circ\text{F}$	869.0	820.7	807.2	731.8
$T_2 - T_3, ^\circ\text{F}$	3.452	3.341	4.754	4.580
$T_3 - T_a, ^\circ\text{F}$	127.5	124.0	188.0	182.6
$T_4 - T_a, ^\circ\text{F}$	38.89	41.22	71.92	77.99
$T_5 - T_4, ^\circ\text{F}$	0.5353	0.5118	1.095	1.057
$T_{\text{max}}, ^\circ\text{F}$	155.0	205.6	208.6	289.1
$x_{T \text{ max}}, \text{ ft}$	0.5851	0.4716	0.6638	0.5484
$\Delta T/H, ^\circ\text{F/ft}$	1.080	1.073	1.688	1.692

Table 6. Results of Investigation of Sixth Steady-State Case

Case Conditions Studied				
	$T_o = 1100^{\circ}\text{F}$		$T_s = 50^{\circ}\text{F}$	
	$L_c = 8 \text{ ft}$			
	$L_s = 1/16 \text{ in.}$	$L_I = 7.5 \text{ in.}$	$L_{FS} = 4 \text{ in.}$	$L_{SS} = 2 \text{ in.}$
	$\phi_o = 1 \times 10^{12} \text{ photons/cm}^2 \cdot \text{sec}$		$\phi_o = 2 \times 10^{12} \text{ photons/cm}^2 \cdot \text{sec}$	
	Bottom of Channel	Top of Channel	Bottom of Channel	Top of Channel
$q_g, \text{ Btu/hr} \cdot \text{ft}^2$	16.57	16.57	33.14	
$q_I, \text{ Btu/hr} \cdot \text{ft}^2$	111.9	111.9	223.8	
$q_{FS}, \text{ Btu/hr} \cdot \text{ft}^2$	338.1	338.1	676.2	
$q_{SS}, \text{ Btu/hr} \cdot \text{ft}^2$	10.69	10.69	21.38	
$q_c, \text{ Btu/hr} \cdot \text{ft}^2$	30.70	30.70	61.40	
$q_c', \text{ Btu/hr} \cdot \text{ft}^2$	23.47	20.35	50.39	
$q_R, \text{ Btu/hr} \cdot \text{ft}^2$	86.60	101.1	164.5	
MWL, Mw	0.2891	0.2649	0.0245	
$T_1, ^{\circ}\text{F}$	1099.9	1099.95	1099.99	
$T_2, ^{\circ}\text{F}$	223.2	265.1	297.9	
$T_3, ^{\circ}\text{F}$	217.2	259.2	288.7	
$T_a, ^{\circ}\text{F}$	100.0	144.0	100.0	
$T_4, ^{\circ}\text{F}$	124.1	170.5	147.2	
$T_5, ^{\circ}\text{F}$	193.6	170.6	147.7	
$T_o - T_1, ^{\circ}\text{F}$	0.0529	0.0488	0.0131	
$T_1 - T_2, ^{\circ}\text{F}$	876.7	834.8	802.1	
$T_2 - T_3, ^{\circ}\text{F}$	6.060	5.931	9.195	
$T_3 - T_a, ^{\circ}\text{F}$	117.2	115.2	188.7	
$T_4 - T_a, ^{\circ}\text{F}$	24.10	26.42	47.24	
$T_5 - T_4, ^{\circ}\text{F}$	0.1965	0.1764	0.4150	
$T_{\text{max}}, ^{\circ}\text{F}$	134.0	177.6	170.7	
$x_T \text{ max, ft}$	0.5375	0.4162	0.6322	
$\Delta T/H, ^{\circ}\text{F/ft}$	0.9177	0.9194	1.532	

Conduction back into reactor room

Table 7. Results of Investigation of Seventh Steady-State Case

Case Conditions Studied				
	$T_o = 1100^\circ\text{F}$	$L_c = 8 \text{ ft}$	$T_e = 50^\circ\text{F}$	
	$L_g = 1/16 \text{ in.}$	$L_I = 10 \text{ in.}$	$L_{FS} = 4 \text{ in.}$	$L_{SS} = 2 \text{ in.}$
	$\phi_o = 1 \times 10^{12} \text{ photons/cm}^2 \cdot \text{sec}$		$\phi_o = 2 \times 10^{12} \text{ photons/cm}^2 \cdot \text{sec}$	
	Bottom of Channel	Top of Channel	Bottom of Channel	Top of Channel
$q_g, \text{ Btu/hr} \cdot \text{ft}^2$	16.57	16.57	33.14	33.14
$q_I, \text{ Btu/hr} \cdot \text{ft}^2$	146.7	146.7	293.4	293.4
$q_{FS}, \text{ Btu/hr} \cdot \text{ft}^2$	307.1	307.1	614.2	614.2
$q_{SS}, \text{ Btu/hr} \cdot \text{ft}^2$	9.689	9.689	19.38	19.38
$q_c, \text{ Btu/hr} \cdot \text{ft}^2$	27.89	27.89	55.78	55.78
$q_c', \text{ Btu/hr} \cdot \text{ft}^2$	21.08	18.35		
$q_R, \text{ Btu/hr} \cdot \text{ft}^2$	73.58	84.92		
MWL, Mw	0.1118	0.0955		
$T_1, ^\circ\text{F}$	1099.98	1099.98		
$T_2, ^\circ\text{F}$	208.6	245.9		
$T_3, ^\circ\text{F}$	203.3	240.7		
$T_a, ^\circ\text{F}$	100.0	138.7		
$T_4, ^\circ\text{F}$	120.9	161.3		
$T_5, ^\circ\text{F}$	121.0	161.5		
$T_o - T_1, ^\circ\text{F}$	0.0232	0.0205		
$T_1 - T_2, ^\circ\text{F}$	891.4	854.1		
$T_2 - T_3, ^\circ\text{F}$	5.304	5.218		
$T_3 - T_a, ^\circ\text{F}$	103.3	102.0		
$T_4 - T_a, ^\circ\text{F}$	20.87	22.59		
$T_5 - T_4, ^\circ\text{F}$	0.1769	0.1594		
$T_{\text{MAX}}, ^\circ\text{F}$	129.6	167.6		
$x_T \text{ max}, \text{ ft}$	0.5256	0.4117		
$\Delta T/H, ^\circ\text{F/ft}$	0.8064	0.8088		

Conduction back into reactor room

Conduction back into reactor room

Tables 1, 6, and 7 may be compared for the effects of changing the thickness of the firebrick insulation from 5 in. to 7.5 in. and 10 in. The addition of 2.5 in. of insulation decreases the conduction loss by about a factor of 2, and this addition also decreases the maximum temperature of the concrete by approximately 15°F in those cases with an incident gamma current of 1×10^{12} photons/cm²·sec.

Tables 1 and 5 may be compared for the effects of changing the total thickness of the steel in the two gamma shields. Decreasing the total thickness from 4 to 2 in. causes only a slight increase in the conduction loss. The maximum temperature of the concrete is increased approximately 10°F for the cases with an incident gamma current of 1×10^{12} photons/cm²·sec and by approximately 20°F for the cases with an incident gamma current of 2×10^{12} photons/cm²·sec.

Tables 1 and 3 and Tables 2 and 4 may be compared for the effects of changing the ratio of the thickness of the steel on the reactor side of the air channel to the thickness of the steel on the concrete side of the air channel. Changing from 4 in. on the reactor side and 2 in. on the concrete side to 2 in. on the reactor side and 4 in. on the concrete side increases the conduction loss only slightly and increases the maximum temperature of the concrete approximately 10°F.

Tables 1 and 2 and Tables 3 and 4 may be compared for the effects of changing the thickness of the concrete and the temperature over the outside surface of the concrete wall. Changing the thickness of the concrete from 8 to 3 ft and the temperature on the outside surface from 50 to 70°F decreases the maximum temperature of the concrete about 10°F but the conduction loss is not affected appreciably.

Case Studied for Transient Condition

Eighteen finite difference equations, with the differencing with respect to time, similar to Eqs. 32 through 35 discussed in Chapter 3 were written to analyze the proposed configuration of the reactor room wall for one transient-condition case. The analysis was performed to

determine the length of time over which a loss of coolant air flow could be tolerated before the temperature of the concrete would exceed the maximum allowable temperature of 212°F. Such a loss of coolant air flow could arise as a result of a malfunction in the blower system supplying the coolant air. Although natural convection currents would cause some circulation of the coolant air during a blower failure, it was assumed that the coolant air was stagnant during the failure so that the worst case could be analyzed. Under this assumption, the air channel serves only as an insulating material and removes no heat from the wall.

The conditions established for the analysis of this particular case were a 5-in.-thick layer of firebrick insulation, a 4-in.-thick layer of mild steel for the first gamma shield, the 3-in.-wide air channel, a 2-in.-thick layer of mild steel for the second gamma shield, and a 6-ft-thick concrete wall for the biological shield. A simple computer program was written to perform the calculations, but the zero-time temperatures and heat depositions for each segment in the composite wall were calculated by hand and used as fixed numbers in the program. This computer program was used only to obtain a first approximation to the transient situation for one particular case, and the details of the program are not presented here.

The program was run for elapsed times of $t = 1.0$ hr, $t = 2.0$ hr, $t = 3.0$ hr, $t = 4.0$ hr, and $t = 5.0$ hr for the condition of internal heat generation (reactor at power during blower failure) during the transient period. The program was then run again for the same elapsed times but for the condition of no internal heat generation (reactor shutdown simultaneous with blower failure) during the transient period. The computer program used to analyze the condition for internal heat generation is given in Table 8. To analyze the condition of no internal heat generation, Q2C through Q19SS in Table 8 are set equal to zero. The resulting temperature distribution in the proposed reactor room wall analyzed for the condition of internal heat generation during the transient period is shown in Fig. 4, and the temperature distribution in the wall with no internal heat generation during the transient period is illustrated in Fig. 5.

Table 8. Computer Program Used to Analyze the Proposed Reactor Room Wall for the Condition of Internal Heat Generation

PROGRAM TSS	
R	= 500.
T	= 0.001
T1	= 26.35
T2A	= 109.65
T3A	= 132.95
T4A	= 156.25
T5A	= 179.42
T6A	= 197.30
T7A	= 186.14
T8A	= 186.04
T9A	= 153.00
T10A	= 290.93
T11A	= 293.03
T12A	= 294.94
T13A	= 296.50
T14A	= 385.98
T15A	= 558.90
T16A	= 724.60
T17A	= 880.72
T18A	= 1030.43
T19A	= 1099.90
T20	= 1100.00
Q2C	= 0.255
Q3C	= 0.255
Q4C	= 0.255
Q5C	= 1.32
Q6C	= 29.99
Q7S	= 2.46
Q8S	= 8.59
Q10S	= 21.11
Q11S	= 49.62
Q12S	= 109.68
Q13S	= 190.84
Q1AS	= 15.09
Q19SS	= 16.57
SIGMA	= 0.000000001719
EPSIL	= 0.7
K	= 1
100	ORAD = (SIGMA/(2./EPSIL-1.))*((T10A+460.)**4-(T8A+460.)**4)
2	T2E = T2A+0.018405*T*(T3A-2.*T2A+T1)+T*0.034083*Q2C
3	T3E = T3A+0.018405*T*(T4A-2.*T3A+T2A)+T*0.034083*Q3C
4	T4E = T4A+0.018405*T*(T5A-2.*T4A+T3A)+T*0.034083*Q4C
5	T5E = T5A+0.018405*T*(T6A-2.*T5A+T4A)+T*0.034083*Q5C
6	T6E = T6A+0.036747*T*(T7A-T6A)+0.018405*T*(T5A-T6A)+T*0.034083*Q6C
7	T7E = T7A+69.6325*T*(T8A-T7A)+0.24062*T*(T6A-T7A)+T*0.223181*Q7S
8	T8E = T8A+0.03107*T*(T9A-T8A)+69.6325*T*(T7A-T8A)+ORAD*T*0.223181
9	T9E = T9A+38.5062*(T10A-2.*T9A+T8A)*T
10	T10E = T10A+69.6325*T*(T11A-T10A)+0.03107*T*(T9A-T10A)+T*0.223181*Q10S
11	T11E = T11A+69.6325*T*(T12A-2.*T11A+T10A)+T*0.223181*Q11S
12	T12E = T12A+69.6325*T*(T13A-2.*T12A+T11A)+T*0.223181*Q12S
13	T13E = T13A+0.79810*T*(T14A-T13A)+69.6325*T*(T12A-T13A)+T*0.223181*Q13S
14	T14E = T14A+3.4744*T*(T15A-T14A)+6.90248*T*(T13A-T14A)+T*1.93022*Q14S

Table 8 (continued)

```

1 CINS
15 T15B = T15A+3.4744*T*(T16A-2.*T15A+T14A)+T*.93022*QINS
16 T16B = T16A+3.4744*T*(T17A-2.*T16A+T15A)+T*.93022*QINS
17 T17B = T17A+3.4744*T*(T18A-2.*T17A+T16A)+T*.93022*QINS
18 TIMEH = T18A+6.93245*T*(T19A-T18A)+3.4744*T*(T17A-T18A)+T*.93022*
1 CINS
19 T19B = T19A+10.7549*T*(T20-T19A)+12.8750*T*(T18A-T19A)+T*3.58483*
1 C19SS
20 V = K
201 TIMEH = V*T
21 TIMEH = TIMEH*.63.
IF(V-K) 29,22,35
30 IF(V=2.*R) 29,22,31
31 IF(V=3.*R) 29,22,32
32 IF(V=4.*R) 29,22,33
33 IF(V=5.*R) 29,22,34
34 IF(V=6.*R) 29,22,35
35 IF(V=7.*R) 29,22,36
36 IF(V=8.*R) 29,22,37
37 IF(V=9.*R) 29,22,38
38 IF(V=10.*R) 29,22,29
22 WRITE(51,1000)(K,TIMEH,TIMEH)
23 WRITE(51,2000)(T1,T2B,T3B,T4B,T5B,T6B,T7B,T8B,T9B,T10B,T11B,T12B,
1 T13B,T14B,T15B,T16B,T17B,T18B,T19B,T20)
24 WRITE(51,3000)(URAD)
IF(V=10.*R) 29,25,25
29 K = K+1
T2A = T2B
T3A = T3B
T4A = T4B
T5A = T5B
T6A = T6B
T7A = T7B
T8A = T8B
T9A = T9B
T10A = T10B
T11A = T11B
T12A = T12B
T13A = T13B
T14A = T14B
T15A = T15B
T16A = T16B
T17A = T17B
T18A = T18B
T19A = T19B
GO TO 100
25 CONTINUE
1000 FORMAT(24HNUMBER OF ITERATIONS = ,I6/24H ELAPSED TIME (HOURS) = ,
1 F10.6/26H ELAPSED TIME (MINUTES) = ,F11.6/??)
2000 FORMAT(36HCELL TEMPERATURES (DEGREES-F)/6H0T1 = ,F8.3,3X,5HT2 = ,
1 F8.3,3X,5HT3 = ,F8.3,3X,5HT4 = ,F8.3,3X,5HT5 = ,F8.3/6H T6 = ,F8.3,
2,3X,5HT7 = ,F8.3,3X,5HT8 = ,F8.3,3X,5HT9 = ,F8.3,3X,5HT10 = ,F8.3/
30H T11 = ,F8.3,3X,5HT12 = ,F8.3,3X,5HT13 = ,F8.3,3X,5HT14 = ,F8.3,3X,
45HT15 = ,F8.3/6H T16 = ,F8.3,3X,5HT17 = ,F8.3,3X,5HT18 = ,F8.3,3X,
55HT19 = ,F8.3,3X,5HT20 = ,F8.3)
3000 FORMAT(8H0GRAD = ,F10.4,15H (BTU/HR-SQ FT))

```

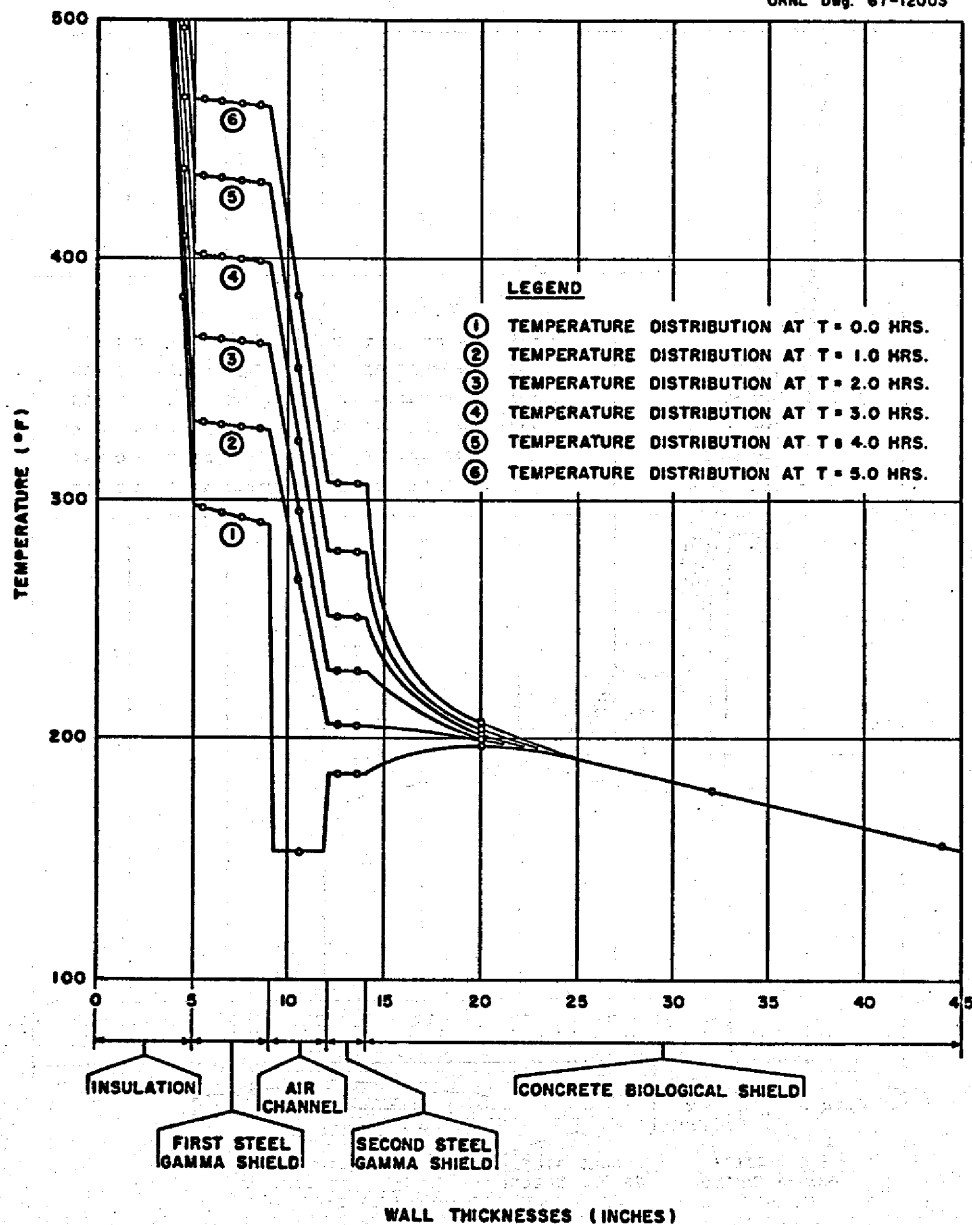


Fig. 4. Temperature Distribution in Proposed Reactor Room Wall With Internal Heat Generation Rate Maintained During Loss-of-Wall-Coolant Transient Period.

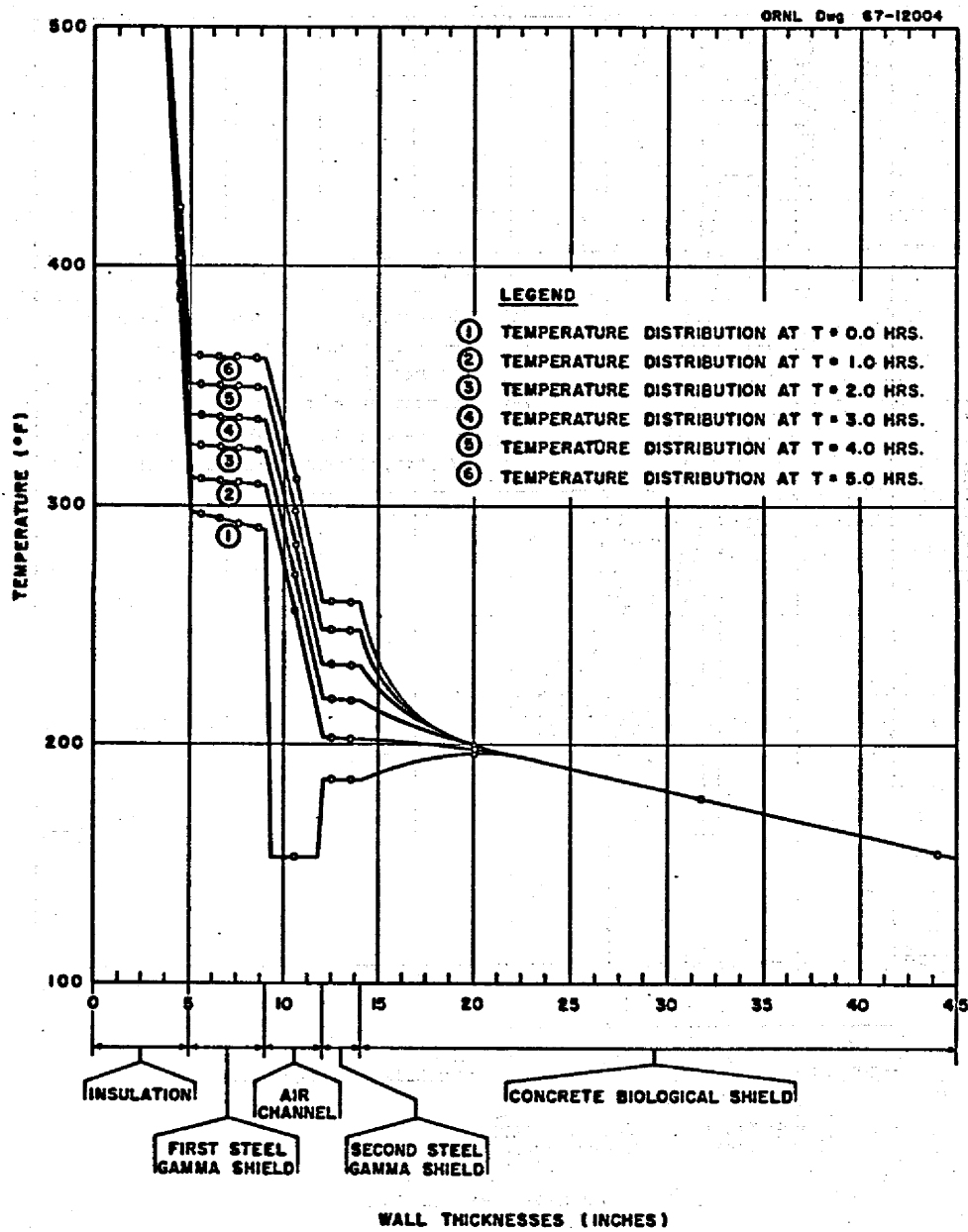


Fig. 5. Temperature Distribution in Proposed Reactor Room Wall With No Internal Heat Generation During the Loss-of-Wall-Coolant Transient Period.

5. CONCLUSIONS

Two basic conclusions may be drawn from the results of the parametric studies made in this investigation of the proposed configuration of a laminated wall to protect the concrete biological shield from the gamma current within the room housing a 250-Mw(e) molten-salt breeder reactor, a fuel-salt-to-coolant-salt heat exchanger, and a blanket-salt-to-coolant-salt heat exchanger. The first basic conclusion is that with air used as the wall coolant, the proposed configuration is acceptable for an incident monoenergetic (1 Mev) gamma current of 1×10^{12} photons/cm²·sec for all cases considered in which the thickness of the firebrick insulation was 5 in. or more. A second basic conclusion is that the proposed configuration is not acceptable for those cases considered with an incident monoenergetic (1 Mev) gamma current of 2×10^{12} photons/cm²·sec because the maximum allowable temperature of the concrete (212°F) is exceeded by 50 to 100°F. The values of several of the parameters of interest in this study that were obtained from the cases analyzed for a gamma current of 1×10^{12} photons/cm²·sec are given in Table 9.

Based on the assumption that the floor and ceiling of the reactor room have the same laminated configuration as the walls, giving a total "wall" surface area of 8276 ft², the proposed wall configuration will allow the conduction loss from the reactor room to be maintained at a level below 1 Mw if the thickness of the insulation is 5 in. or more. Further, based on an air velocity of 50 ft/sec and an air coolant channel width of 3 in., air is an acceptable medium for cooling the wall.

A general conclusion that may be drawn from the limited analysis made of one transient-condition case is that if the ambient temperature of the reactor room remains at approximately 1100°F, the proposed configuration of the reactor room wall studied in this case can sustain a loss of coolant air flow under the conditions described in Chapter 4 for approximately 1 hour before the temperature of the concrete begins to exceed 212°F. If a zero incident gamma current is assumed, the "permissible" loss-of-coolant-air time is greater than one hour but less than two hours.

Table 9. Range of Parameters of Interest in Studies Made of Proposed Wall With An Incident Gamma Current of 1×10^{12} photons/cm²·sec

Variable of Interest	Minimum Value	Maximum Value	Parametric Conditions				
			L _I (in.)	L _{FS} (in.)	L _{SS} (in.)	L _c (ft)	T _B (°F)
Skin ΔT , °F	0.021		10	4	2	a	a
		0.22	2.5	2	4	a	a
Insulation ΔT , °F	726		2.5	4	2	8	50
		906	10	2	a	a	a
First steel shield ΔT , °F	2.38		10	2	a	a	a
		10.9	2.5	4	2	a	a
Second steel shield ΔT , °F	0.08		2.5	4	2	3	70
		1.1	2.5	2	4	8	50
Air vertical temperature gradient, °F/ft	0.77		10	2	2	3	70
		1.57	2.5	4	2	8	50
T _{c max} , °F ($< 212^\circ\text{F}$)	124		10	4	2	3	70
		205.6	5	2	2	8	50
x _{T max} , ft (T _{max} $< 212^\circ\text{F}$)	0.11		5	2	4	3	70
		0.58	7.5	2	2	8	50
MWL, Mw	0.096		10	4	2	8	50
		1.32	2.5	2	a	a	a

^aThis parameter has little effect in combination with the other parameters given, and the values of the variables of interest are essentially the same for various values of this parameter.

If a wall of the type proposed is used, the temperature of the concrete, T_c , or the conduction loss, or both, can be controlled to some extent by varying the physical characteristics of the wall. The thickness of the insulation can be increased, but the desirable effect approaches a limit rather rapidly. As the results of our parametric studies have indicated, an insulation thickness can be reached that will cause conduction back into the reactor room. The total thickness of the mild-steel gamma shields can be increased with good results up to the point where the gamma current is reduced by several orders of magnitude. After this point is reached, adding more steel for gamma shielding does not produce sizable changes in the maximum temperature of the concrete. A total of approximately 6 in. of steel is sufficient for an incident monoenergetic (1 Mev) gamma current of 1×10^{12} photons/cm²·sec. The thickness of the mild-steel gamma shields should be arranged so that the major portion of the steel is on the reactor side of the air channel. Placing the major portion of the steel on the concrete side of the air channel results in the undesirable effect of raising the maximum temperature of the concrete. Shadow shielding of the particular components within the reactor room that may be causing a large gamma current appears to be a better solution than increasing the thickness of the wall laminations for gamma currents greater than 1×10^{12} photons/cm²·sec.

When sufficient information becomes available, an overall energy balance should be written, starting with the fissioning process in the reactor and extending out through the wall of the reactor room to an outside surface. This balance is necessary to determine whether or not a conduction loss of 1 Mw will permit maintenance of the desired ambient temperature within the reactor room without the addition of auxiliary cooling or heating systems.

The first part of the document discusses the importance of maintaining accurate records of all transactions. It emphasizes that every entry should be supported by a valid receipt or invoice. This ensures transparency and allows for easy verification of the data.

In the second section, the author outlines the various methods used to collect and analyze the data. This includes both primary and secondary data collection techniques. The primary data was gathered through direct observation and interviews, while secondary data was obtained from existing reports and databases.

The third section details the statistical analysis performed on the collected data. This involves the use of descriptive statistics to summarize the data and inferential statistics to test hypotheses. The results of these analyses are presented in a clear and concise manner, highlighting the key findings of the study.

Finally, the document concludes with a discussion of the implications of the findings. It suggests that the results have significant implications for the field of study and provides recommendations for further research. The author also acknowledges the limitations of the study and offers suggestions for how these can be addressed in future work.

APPENDICES

.C

.C

Appendix A

EQUATIONS NECESSARY TO CONSIDER A MULTIENERGETIC GAMMA CURRENT

The equations derived in Chapter 3 of this report were based on the assumption that the incident gamma current is monoenergetic. If the energy distribution of the incident gamma current is known, this current can be represented as a multigroup current. The equations in which an incident multigroup gamma current appears, either directly or indirectly, must be written to account for this segmentation in gamma energy. This multigroup modification has been made in the following equations, and they are to be used in place of the correspondingly numbered equations in Chapter 3 when the energy distribution of the gamma current is known. The subscript i denotes the energy group, and the terms are defined in Appendix E.

$$Q(x) = \sum_i Q_{o_i} \left[A_i e^{\alpha_i \mu_i x} + (1 - A_i) e^{-\beta_i \mu_i x} \right] e^{-\mu_i x}. \quad (\text{A.8})$$

$$Q(x) = \sum_i Q_{o_i} \left[A_i e^{\mu_i x (\alpha_i - 1)} + (1 - A_i) e^{-\mu_i x (\beta_i + 1)} \right]. \quad (\text{A.9})$$

$$Q_o = \sum_i E_i \bar{\phi}_o \mu_{E_i}. \quad (\text{A.9a})$$

$$T(x) = T_o + \frac{x}{L} (T_L - T_o)$$

$$\begin{aligned} & + \sum_i \frac{Q_{o_i}}{k \mu_i^2} \left\{ \left[\frac{A_i}{(\alpha_i - 1)^2} \left(1 - e^{\mu_i x (\alpha_i - 1)} \right) \right. \right. \\ & \quad \left. \left. + \frac{(1 - A_i)}{(\beta_i + 1)^2} \left(1 - e^{-\mu_i x (\beta_i + 1)} \right) \right] \right. \\ & \left. - \frac{x}{L} \left[\frac{A_i}{(\alpha_i - 1)} \left(1 - e^{\mu_i L (\alpha_i - 1)} \right) + \frac{1 - A_i}{(\beta_i + 1)} \left(1 - e^{-\mu_i L (\beta_i + 1)} \right) \right] \right\} \end{aligned} \quad (\text{A.12})$$

$$\begin{aligned} \frac{dT}{dx} &= \frac{1}{L}(T_L - T_0) \\ &+ \sum_i \frac{Q_{o_i}}{k\mu_i^2} \left\{ \left[\frac{A_i \mu_i}{(\alpha_i - 1)} \left(-e^{\mu_i x (\alpha_i - 1)} \right) + \frac{\mu_i (1 - A_i)}{\beta_i + 1} \left(+e^{-\mu_i x (\beta_i + 1)} \right) \right] \right. \\ &\left. - \frac{1}{L} \left[\frac{A_i}{(\alpha_i - 1)^2} \left(1 - e^{\mu_i L (\alpha_i - 1)} \right) + \frac{1 - A_i}{(\beta_i + 1)^2} \left(1 - e^{-\mu_i L (\beta_i + 1)} \right) \right] \right\} \quad (A.13) \end{aligned}$$

$$\begin{aligned} &\sum_i \left[\frac{Q_{o_i} (1 - A_i)}{\mu_i k (\beta_i + 1)} e^{-\mu_i x (\beta_i + 1)} - \frac{Q_{o_i} A_i}{\mu_i k (\alpha_i - 1)} e^{\mu_i x (\alpha_i - 1)} \right] \\ &= \frac{1}{L}(T_0 - T_L) + \sum_i \frac{Q_{o_i}}{k\mu_i} \left\{ \frac{1}{L} \left[\frac{A_i}{(\alpha_i - 1)^2} \left(1 - e^{\mu_i L (\alpha_i - 1)} \right) \right. \right. \\ &\quad \left. \left. + \frac{(1 - A_i)}{(\beta_i + 1)^2} \left(1 - e^{-\mu_i L (\beta_i + 1)} \right) \right] \right\} . \quad (A.14) \end{aligned}$$

$$q_T = \sum_i \left\{ \int_0^L Q_{o_i} \left[A_i e^{\mu_i x (\alpha_i - 1)} + (1 - A_i) e^{-\mu_i x (\beta_i + 1)} \right] dx \right\} . \quad (A.16)$$

$$q_T = \sum_i \left\{ \frac{Q_{o_i}}{\mu_i} \left[\frac{A_i}{(\alpha_i - 1)} \left(e^{\mu_i L (\alpha_i - 1)} - 1 \right) - \frac{(1 - A_i)}{(\beta_i + 1)} \left(e^{-\mu_i L (\beta_i + 1)} - 1 \right) \right] \right\} . \quad (A.17)$$

$$q_{j+1_i} = q_{o(j)_i} - q_{j_i} ,$$

$$q_{j+1} = \sum_i q_{j+1_i} = \sum_i (q_{o(j)_i} - q_{j_i}) . \quad (A.18)$$

$$q_{o(j)_i} = \left(\frac{Q_{o(j)}}{\mu_{E(j)}} \right)_i ,$$

$$q_{o(j)} = \sum_i q_{o(j)_i} = \sum_i \left(\frac{Q_{o(j)}}{\mu_{E(j)}} \right)_i , \quad (A.18a)$$

$$Q_o(j+1)_i = (q_o(j+1)_i)^{\mu_{E(j+1)_i}},$$

$$Q_o(j+1) = \sum_i Q_o(j+1)_i = \sum_i (q_o(j+1)_i)^{\mu_{E(j+1)_i}}. \quad (\text{A.18b})$$

$$\begin{aligned} \left. \frac{dT}{dx} \right|_{x=0} &= \frac{1}{L_c} (T_6 - T_5) + \sum_i \frac{Q_{o_i}}{k_c \mu_i^2} \left\{ \left[-\frac{A_i \mu_i}{(\alpha_i - 1)} + \frac{\mu_i (1 - A_i)}{(\beta_i + 1)} \right] \right. \\ &\quad - \frac{1}{L_c} \left[\frac{A_i}{(\alpha_i - 1)^2} (1 - e^{\mu_i L_c (\alpha_i - 1)}) \right. \\ &\quad \left. \left. + \frac{(1 - A_i)}{(\beta_i + 1)^2} (1 - e^{-\mu_i L_c (\beta_i + 1)}) \right] \right\}. \quad (\text{A.27}) \end{aligned}$$

$$\begin{aligned} &\left(\frac{\sigma}{\epsilon - 1} \right) T_4^4 + T_4 \left(h + \frac{1}{\frac{L_{SS}}{k_{SS}} + \frac{L_c}{k_c}} \right) \\ &= \left(\frac{\sigma}{\epsilon - 1} \right) T_3^4 + h T_a + q_{SS} + \frac{T_6 + \frac{L_c}{k_c} \sum_i \left[\left(\frac{Q_o(c)_i}{\mu_i^2} \right) B'_i \right] - \frac{2L_{SS} q_{SS}}{3k_{SS}}}{\frac{L_{SS}}{k_{SS}} + \frac{L_c}{k_c}}, \quad (\text{A.29}) \end{aligned}$$

where

$$\begin{aligned} B'_i &= \left(\frac{\mu_i (1 - A_i)}{(\beta_i + 1)} - \frac{\mu_i A_i}{(\alpha_i - 1)} \right) - \frac{1}{L} \left[\frac{A_i}{(\alpha_i - 1)^2} (1 - e^{\mu_i L_c (\alpha_i - 1)}) \right. \\ &\quad \left. + \frac{(1 - A_i)}{(\beta_i + 1)^2} (1 - e^{-\mu_i L_c (\beta_i + 1)}) \right]. \end{aligned}$$

Appendix B

EVALUATION OF THE CONVECTIVE HEAT TRANSFER COEFFICIENT

The average convective heat transfer coefficient, h , for the walls of the air channel was evaluated by using the expression published by Kreith.¹

$$h = 0.036 \frac{k}{H} Re_H^0.8 Pr^{1/3},$$

where

k = thermal conductivity of air, Btu/hr·ft·°F,

H = vertical length of the air channel, ft,

Re_H = Reynolds number evaluated at the top of the air channel, and

Pr = Prandtl number evaluated for air.

The Reynolds number evaluated at the top of the air channel,

$$Re_H = \frac{U\rho H}{\mu},$$

where

U = the bulk air velocity, ft/sec,

ρ = density of the air, lb/ft³, and

μ = viscosity of air, lb/ft·sec.

The Prandtl number evaluated for air,

$$Pr = \frac{\mu C_p}{k},$$

where C_p = the specific heat of air at a constant pressure, Btu/lb·°F.

In the range of temperatures considered, Pr is approximately constant and equal to 0.72. Kreith's¹ expression for h was evaluated for various air-wall mean temperatures in the air channel, and the results are on the following page.

¹ Frank Kreith, p. 286 in Principles of Heat Transfer, International Textbook Company, Scranton, Pennsylvania, 4th printing, 1961.

\bar{T} (°F)	h (Btu/hr·ft ² ·°F)
100	5.15
130	5.04
150	5.04

The mean temperature of the walls of the air channel is expected to be approximately 130 to 150°F, and a value of 5 was used for the convective heat transfer coefficient at the walls of the air channel.

Appendix C

VALUES OF PHYSICAL CONSTANTS USED IN THIS STUDY

Values for the gamma energy attenuation coefficient, μ_E , the total gamma attenuation coefficient, μ , and the dimensionless constants α , β , and A used in the Taylor buildup formula for a gamma energy of 1 Mev are tabulated below.

Material	μ_E (ft ⁻¹)	μ (ft ⁻¹)	α	β	A
Type 347 stainless steel	6.28 ^a	14.08 ^b	0.0895 ^c	0.04 ^c	8 ^c
Kaolin insulating brick	0.367 ^d	0.838 ^d	0.088 ^d	0.029 ^d	10 ^d
Mild steel	6.30 ^a	14.02 ^a	0.0895 ^c	0.04 ^c	8 ^c
Concrete	1.99 ^d	4.55 ^d	0.088 ^d	0.029 ^d	10 ^d

Values for the density, ρ , specific heat, C_p , thermal conductivity, k , and equivalent thermal conductivity at interfaces of adjacent materials, \bar{k} , for materials in the proposed laminated wall in their order of occurrence from the reactor outward are tabulated below.

Material	ρ (g/cm ³)	ρ (lb _m /ft ³)	C_p (Btu/lb _m ·°F)	k (Btu/hr·ft·°F)	\bar{k} (Btu/hr·ft·°F)
Type 347 stainless steel	7.8 ^b	486.9 ^b	0.11 ^e	12.8 ^e	0.159
Kaolin insulating brick	0.433 ^e	27.03 ^e	0.23 ^e	0.15 ^e	0.298
Mild steel	7.83 ^b	488.8 ^b	0.11 ^e	26.0 ^e	0.0232
Air		0.060 ^e	0.241 ^e	0.0174 ^e	0.0232
Mild steel	7.83 ^b	488.8 ^b	0.11 ^e	26.0 ^e	0.584
Concrete	2.35 ^d	146.7 ^d	0.20 ^e	0.54 ^e	

^aE. P. Blizard and L. S. Abbott, editors, p. 107 in Reactor Handbook, Vol. 3, Part B, John Wiley and Sons, New York, 1962.

^bM. M. El-Wakil, p. 223 in Nuclear Power Engineering, McGraw-Hill Book Company, Inc., First Edition, New York, New York, 1962.

^cE. P. Blizard and L. S. Abbott, editors, p. 116 in Reactor Handbook, Vol. 3, Part B, John Wiley and Sons, New York, 1962.

^d"Reactor Physics Constants," USAEC Report ANL-5800, Argonne National Laboratory, pp. 653-657, July 1963.

^eFrank Kreith, pp. 533-535 in Principles of Heat Transfer, International Textbook Company, 4th printing, Scranton, Pennsylvania, 1961.

Appendix D

TSS COMPUTER PROGRAM

A program was developed for the CDC 1604-A computer to solve the equations (Eqs. 8 through 31) necessary to evaluate the proposed configuration of the reactor room wall for the steady-state conditions. As written, the TSS (Thermal Shield Study) program will handle up to five material laminations, excluding the air channel, and up to eight energy groups for the incident gamma current. The calculations are performed in the order described in Chapter 3. For a problem with five energy groups and sixteen different combinations of laminations (cases), the machine time is one minute and 45 seconds and the compilation time is 56 seconds.

A Newton-Raphson iteration scheme is used to evaluate T_4 and $x_{T \max}$. The convergence criterion for T_4 is that the right and left sides of Eq. 29 must agree to within 0.05, and the criterion for $x_{T \max}$ is that the right and left sides of Eq. 14 must agree to within 0.10. These convergence criteria could be made smaller with a corresponding increase in machine time, but very little more real accuracy would be obtained because the program uses the approximate method to calculate the incident gamma current at each material interface. If more real accuracy is required, the program could be modified to calculate the attenuated gamma current at each interface and to calculate from this information the incident gamma current at the material interfaces.

If a vertical temperature profile were known for the interface of the reactor room and the skin, the program could be modified to do calculations at several points up the air channel rather than just at the top and bottom as it does at present. Both the setup of the program and the manner in which the necessary input data are prepared are explained in the following discussion.

The TSS computer program is set up for a given physical situation with a given photon current incident upon the reactor room wall. The temperature of the inside surface of the wall is fixed at a given value.

The composite wall is composed of five material regions, and progressing from the inside surface outward, these regions are (1) a thin steel skin, (2) an insulating material, (3) the first steel gamma shield, (4) the second steel gamma shield, and (5) the concrete biological shield with a fixed temperature on the outside surface. The 3-in.-wide air channel placed between the first and second gamma shields is not considered a material region. By calculating a vertical temperature gradient in the air channel, the program will calculate at both the bottom and top of the reactor room wall the

1. gamma heat generation rate in each material,
2. temperature at each material interface and temperature changes across each material,
3. conduction heat loss from the reactor room to the air channel,
4. radiation heat transfer rate between the walls of the air channel,
5. heat in the concrete conducted both toward and away from the air channel, and the
6. maximum temperature in the concrete and its corresponding location.

The program input deck allows the use of any material in any region of the composite wall. For a fixed incident photon current, a fixed inside wall temperature, a fixed inlet air velocity and temperature, and fixed wall materials, the calculation of a particular case is done by selecting all material thicknesses and the temperature of the outside surface of the concrete wall. At present, the program will allow a maximum of 32 cases to be run, but it can easily be expanded to handle more.

Preparation of Input Data

The first set of input data consists of energy-dependent information pertaining to the incident photon current and to the nuclear properties of the materials chosen for each region in the wall. The order in which the information is supplied is given on the following page.

Card 1. QS1(1), QS1(2), ..., QS1(8). The incident photon current (Btu/hr·ft²) for each of eight possible energy groups.

Card 2. EMU1(1), EMU1(2), ..., EMU1(8). The energy absorption coefficient (1/ft) in the first region of the wall (the inner skin) for each of eight possible energy groups.

Card 3. AMU1(1), AMU1(2), ..., AMU1(8). The mass attenuation coefficient (1/ft) in the first region of the wall (the inner skin) for each of eight possible energy groups.

Card 4. ALPHA(1), ALPHA1(2), ..., ALPHA1(8). The dimensionless constant α used in the Taylor buildup formula in the first region of the wall (the inner skin) for each of eight possible energy groups.

Card 5. BETA1(1), BETA1(2), ..., BETA1(8). The dimensionless constant β used in the Taylor buildup formula in the first region of the wall (the inner skin) for each of eight possible energy groups.

Card 6. A1(1), A1(2), ..., A1(8). The dimensionless constant A used in the Taylor buildup formula in the first region of the wall (the inner skin) for each of eight possible energy groups.

Card 7. EMU2(1), EMU2(2), ..., EMU2(8). The same as Card 2 except for the second region of the wall (insulation).

Card 8. AMU2(1), AMU2(2), ..., AMU2(8). The same as Card 3 except for the second region of the wall (insulation).

Card 9. ALPHA2(1), ALPHA2(2), ..., ALPHA2(8). The same as Card 4 except for the second region of the wall (insulation).

Card 10. BETA2(1), BETA2(2), ..., BETA2(8). The same as Card 5 except for the second region of the wall (insulation).

Card 11. A2(1), A2(2), ..., A2(8). The same as Card 6 except for the second region of the wall (insulation).

Card 12. EMU3(1), EMU3(2), ..., EMU3(8). The same as Card 2 except for the third region of the wall (the first gamma shield).

Card 13. AMU3(1), AMU3(2), ..., AMU3(8). The same as Card 3 except for the third region of the wall (the first gamma shield).

Card 14. ALPHA3(1), ALPHA3(2), ..., ALPHA3(8). The same as Card 4 except for the third region of the wall (the first gamma shield).

Card 15. BETA3(1), BETA3(2), ..., BETA3(8). The same as Card 5 except for the third region of the wall (the first gamma shield).

Card 16. A3(1), A3(2), ..., A3(8). The same as Card 6 for the third region of the wall (the first gamma shield).

Card 17. EMU4(1), EMU4(2), ..., EMU4(8). The same as Card 2 except for the fourth region of the wall (the second gamma shield).

Card 18. AMU4(1), AMU4(2), ..., AMU4(8). The same as Card 3 except for the fourth region of the wall (the second gamma shield).

Card 19. ALPHA4(1), ALPHA4(2), ..., ALPHA4(8). The same as Card 4 except for the fourth region of the wall (the second gamma shield).

Card 20. BETA4(1), BETA4(2), ..., BETA4(8). The same as Card 5 except for the fourth region of the wall (the second gamma shield).

Card 21. A4(1), A4(2), ..., A4(8). The same as Card 6 except for the fourth region of the wall (the second gamma shield).

Card 22. EMU5(1), EMU5(2), ..., EMU5(8). The same as Card 2 except for the fifth region of the wall (the biological shield).

Card 23. AMU5(1), AMU5(2), ..., AMU5(8). The same as Card 3 except for the fifth region of the wall (the biological shield).

Card 24. ALPHA5(1), ALPHA5(2), ..., ALPHA5(8). The same as Card 4 except for the fifth region of the wall (the biological shield).

Card 25. BETA5(1), BETA5(2), ..., BETA5(8). The same as Card 5 except for the fifth region of the wall (the biological shield).

Card 26. A5(1), A5(2), ..., A5(8). The same as Card 6 except for the fifth region of the wall (the biological shield).

The format statement for all of the above cards is 8F9.0. Since only the first 72 spaces on each data card are used, the last eight may be used for identification purposes. If fewer than eight energy groups are used, the unused data fields may either be punched with a zero or left blank. In either case, the energy-summing DO loops subscripted J, K, L, and N must be changed to correspond to the number of energy groups used; that is, if there are six energy groups, DO 100 I = 1,6; and K, L, and N are also 1,6. If the DO loops are not changed to correspond to the number of energy groups used, division by zero will occur.

The next set of data entered is energy independent and is assumed to be constant over the range of temperatures covered in the program. This information should be given on the two following cards.

Card 27. CON1, CON2, CON3, CON4, CON5, T0, HT, and HF. The thermal conductivities (Btu/hr·ft·°F) of the materials in each of the five regions should be entered in the first five data fields. The temperature on the inside surface of the reactor room wall, T0 in °R, the height of the reactor room, HT in ft, and the film coefficient on the sides of the air channel, HF in Btu/hr·ft²·°F, should be entered in data fields six through eight. The format for this card is the same as that for the previous 26 cards (8F9.0).

Card 28. TA, EPSIL, VEL, ACHAN, CP, RHO, and SIGMA are respectively the inlet air temperature, °R, the emissivity of the surface of the air channel (dimensionless and assumed to be equal for both sides of the air channel), the velocity of the air, ft/sec, the width of the air channel, ft², the specific heat of air, Btu/lb·°F, the density of air, lb/ft³, and the Stefan-Boltzmann constant (Btu/hr·ft²·°R⁴). These values must be entered according to format 6F9.0, F18.0. Again, the last eight spaces can be used for identification.

Preparation of Case Data

Once the input data have been supplied, one card must be prepared for each case to be run. This card contains EL1, EL2, EL3, EL4, EL5, and T6. EL1 through EL5 correspond to the material thicknesses (ft) to be used for each of the five regions in the wall, and T6 is the temperature of the external surface of the concrete biological shield in °R. The format 8F9.0 allows nine spaces for each data field and the last eight spaces for identification. For 16 cases, the cards could be numbered 29 through 44. Numbering is for the user's convenience and is not required. The first DO loop in the program must always be changed to DO 5000 I = 1,N where N is the number of cases to be run. All cases must have the same air temperature, TA, and the statement immediately

following DO 5000 I = 1,N must be written to correspond to the air temperature used. The DIMENSION statement containing EL1(I) through EL5(I), T6(I), BOP(I), and BAM(I) must be checked to see that a sufficient dimension size is given to allow all of the cases to be run. BOP(I) and BAM(I) are dummy variables and may be left blank.

Typical Computer Sheets

The assembly of the control cards, deck, input data, and case data cards for the TSS computer program is illustrated in Fig. D.1. Typical data for 32 cases to be run with one energy group are given in Table D.1. The output data at the bottom of the air channel for one case are given in Table D.2, and the output data at the top of the air channel for the case are given in Table D.3.

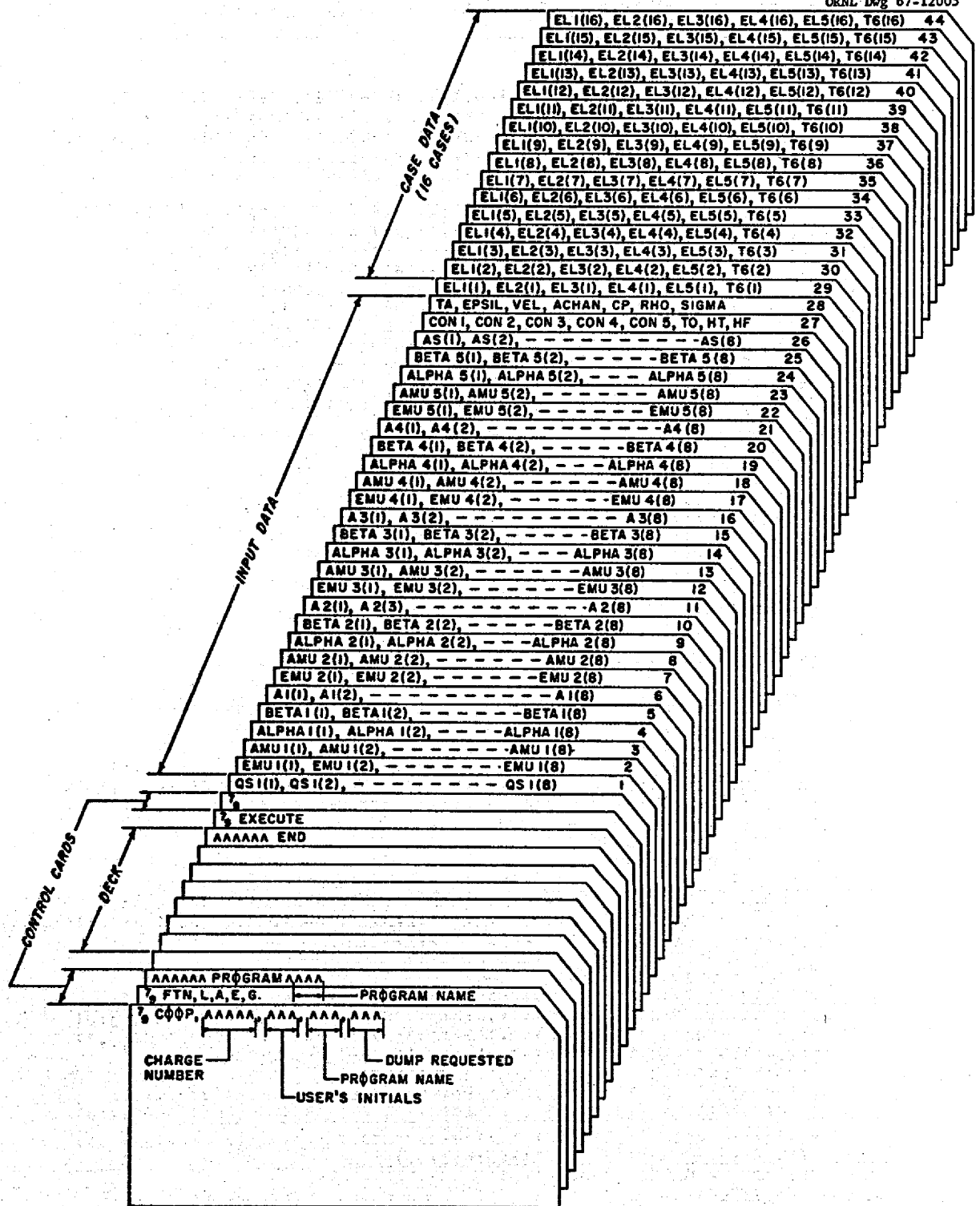


Fig. D.1. Assembly of Data Cards for TSS Computer Program.

Table D.1. Typical Data for 32 Cases With One Energy Group for the TSS Computer Program

```

PROGRAM TSS
DIMENSION QDPTS(6)
DIMENSION QS1(8), EMU1(8), AMU1(8), ALPHA1(8), BETA1(8), A1(8),
EMU2(8), AMU2(8), ALPHA2(8), BETA2(8), A2(8), EMU3(8), AMU3(8),
ALPHA3(8), BETA3(8), A3(8), EMU4(8), AMU4(8), ALPHA4(8), BETA4(8),
A4(8), EMU5(8), AMU5(8), ALPHA5(8), BETA5(8), A5(8)
DIMENSION EL1(32), EL2(32), EL3(32), EL4(32), EL5(32), T6(32),
IBOP(32), BAM(32)
DIMENSION QDEP1(6), QS2(6), QV1(6), QV2(6), QDEP2(6), QS3(6),
QV3(6), QDEP3(6), QS4(6), QV4(6), QDEP4(6), QS5(6), QV5(6),
QDEP5(6), B(6), D1(6), E1(6), D2(6), E2(6), F1(6), F2(6), F3(6),
F4(6), SUM(6), SUMP(6), R1(6), RE1(6), R2(6), RE2(6)
READ (50, 1000) (QS1, EMU1, AMU1, ALPHA1, BETA1, A1,
EMU2, AMU2, ALPHA2, BETA2, A2, EMU3, AMU3, ALPHA3, BETA3, A3,
BETA4, A4, EMU5, AMU5, ALPHA5, BETA5, A5)
READ (50, 1001) (TA, EPSIL, VEL, ACHAN, CP, RHO, SIGMA)
READ (50, 1000) (EL1(1), EL2(1), EL3(1), EL4(1), EL5(1), T6(1),
IBOP(1), BAM(1), I=1:32)
C BEGIN MAIN PROGRAM
DO 5000 I=1,32
TA = 560.
ELX1 = EL1(I)
ELX2 = EL2(I)
ELX3 = EL3(I)
ELX4 = EL4(I)
ELX5 = EL5(I)
T6X = T6(I)
QDEPT1 = 0.
QDEPT2 = 0.
QDEPT3 = 0.
QDEPT4 = 0.
QDEPT5 = 0.
C CALCULATION OF SOURCE TERM AND GAMMA HEAT DEPOSITION TERMS
DO 100 J = 1,1
1 QV1(J) = QS1(J)*EMU1(J)
2 QDEP1(J) = QV1(J)*(((A1(J)*EXPF(AMU1(J)*ELX1*(ALPHA1(J)-1.)))/
1(AMU1(J)*(ALPHA1(J)+1.))-((1.-A1(J))*EXPF(-AMU1(J)*ELX1*(BETA1(J)+
2.)))/(AMU1(J)*(BETA1(J)+1.)))-((A1(J))/(AMU1(J)*(ALPHA1(J)-1.))-
3((1.-A1(J))/(AMU1(J)*(BETA1(J)+1.))))
3 QS2(J) = QS1(J)+QDEP1(J)
4 QV2(J) = QS2(J)*EMU2(J)
5 QDEP2(J) = QV2(J)*(((A2(J)*EXPF(AMU2(J)*ELX2*(ALPHA2(J)-1.)))/
1(AMU2(J)*(ALPHA2(J)+1.))-((1.-A2(J))*EXPF(-AMU2(J)*ELX2*(BETA2(J)+
2.)))/(AMU2(J)*(BETA2(J)+1.)))-((A2(J))/(AMU2(J)*(ALPHA2(J)-1.))-
3((1.-A2(J))/(AMU2(J)*(BETA2(J)+1.))))
6 QS3(J) = QS1(J)+QDEP1(J)+QDEP2(J)
7 QV3(J) = QS3(J)*EMU3(J)
8 QDEP3(J) = QV3(J)*(((A3(J)*EXPF(AMU3(J)*ELX3*(ALPHA3(J)-1.)))/
1(AMU3(J)*(ALPHA3(J)+1.))-((1.-A3(J))*EXPF(-AMU3(J)*ELX3*(BETA3(J)+
2.)))/(AMU3(J)*(BETA3(J)+1.)))-((A3(J))/(AMU3(J)*(ALPHA3(J)-1.))-
3((1.-A3(J))/(AMU3(J)*(BETA3(J)+1.))))
ELX4 = ELX4+ELX3
QDPTS(J) = QV3(J)*(((A4(J)*EXPF(AMU4(J)*ELX4*(ALPHA4(J)-1.)))/
1(AMU4(J)*(ALPHA4(J)+1.))-((1.-A4(J))*EXPF(-AMU4(J)*ELX4*(BETA4(J)+
2.)))/(AMU4(J)*(BETA4(J)+1.)))-((A4(J))/(AMU4(J)*(ALPHA4(J)-1.))-
3((1.-A4(J))/(AMU4(J)*(BETA4(J)+1.))))
QDEP4(J) = QDPTS(J)+QDEP3(J)
ELX4 = ELX4+ELX3
12 QS5(J) = QS1(J)+QDEP1(J)+QDEP2(J)+QDEP3(J)+QDEP4(J)
13 QV5(J) = QS5(J)*EMU5(J)
14 QDEP5(J) = QS5(J)
15 QDEPT1 = QDEPT1+QDEP1(J)
16 QDEPT2 = QDEPT2+QDEP2(J)

```


Table D.1 (continued)

```

17 QDEPT3 = QDEPT3+QDEP3(J)
18 QDEPT4 = QDEPT4+QDEP4(J)
19 QDEPT5 = QDEPT5+QDEP5(J)
100 CONTINUE
20 K7=0
C BEGIN CALCULATION FOR THE REACTOR SIDE OF THE CHANNEL
21 QCON = ((T0-TA)-QDEPT1*(2.*ELX1/(3.*CON1)+ELX2/CON2+ELX3/CON3+1./
  HF)-QDEPT2*(2.*ELX2/(3.*CON2)+ELX3/CON3+1./HF)-QDEPT3*(2.*ELX3/
  2(3.*CON3)+1./HF))/(ELX1/CON1+ELX2/CON2+ELX3/CON3+1./HF)
22 DELT1 = (QCON+2.*QDEPT1/3.)*ELX1/CON1
C (NC CARD NO. 23)
24 T0F = T0-460.
25 T1F = T0F-DELT1
26 DELT2 = (QCON+QDEPT1+2.*QDEPT2/3.)*ELX2/CON2
27 T2F = T1F-DELT2
28 DELT3 = (QCON+QDEPT1+QDEPT2+2.*QDEPT3/3.)*ELX3/CON3
29 T3F = T2F-DELT3
30 DELT4 = (QCON+QDEPT1+QDEPT2+QDEPT3)/HF
31 TAF = TA-460.
C CHECK FOR UNACCEPTABLE HEAT CONDUCTION CONDITIONS
32 IF(QCON) 3005,33,33
33 CONTINUE
34 IF(DELT1) 3005,35,35
35 CONTINUE
36 IF(DELT2) 3005,37,37
37 CONTINUE
38 IF(DELT3) 3005,39,39
39 CONTINUE
40 IF(DELT4) 3005,41,41
41 CONTINUE
42 BT = 0.
C BEGIN CALCULATION FOR THE CONCRETE SIDE OF THE CHANNEL
43 DO 200 K=1,1
44 B(K) = (DV5(K)/(AMU5(K)**2))*(((AMU5(K)*(1.+A5(K)))/(1.+BETA5(K))
  1-(AMU5(K)*A5(K))/(ALPHA5(K)-1.))-((1./ELX5)*((A5(K)/(ALPHA5(K)-1.)
  2**2)*(1.-EXPF(AMU5(K)*ELX5*(ALPHA5(K)-1.)))+(1.-A5(K))/(1.+
  3BETA5(K)**2)))+(1.-EXPF(-AMU5(K)*ELX5*(1.+BETA5(K))))))
45 BT = BT+B(K)
200 CONTINUE
46 CF1 = SIGMA/(2./EPS)L=1.)
47 CF2 = HF+1./((ELX4/CON4+ELX5/CON5)
48 CF3 = (T6X+ELX5*BT/CON5+2.*ELX4*QDEPT4/(3.*CON4))/(ELX4/CON4+ELX5/
  CON5)
49 K9 = 0
C ITERATION PROCESS FOR T4
50 T4 = TA
51 T3 = T3F+460.
52 FT4 = CF1*(T4**4)+CF2*T4+CF1*(T3**4)+HF*TA-QDEPT4-CF3
53 FT4P = 4.*CF1*(T4**3)+CF2
54 IF(ABS(FT4)-0.05) 58,58,55
55 T4 = T4+FT4/FT4P
56 K9 = K9+1
57 GO TO 51
58 CONTINUE
59 QRAD = CF1*(T3**4-T4**4)
60 QCCP = HF*(T4-TA)-QDEPT4-QRAD
61 DELT5 = (T4-TA)
62 DELT6 = (ELX4*QCCP/CON4)+2.*ELX4*QDEPT4/(3.*CON4)
63 T4F = T4-460.
64 T5 = T4+DELT6
65 T5F = T5-460.
66 T6XF = T6X-460.
C (NC CARD NUMBERS 67-70)
71 X = 0.
72 K3 = 0
73 FT = 0.

```

Table D.1 (continued)

```

74 SUMT = 0.
75 SUMPT = 0.
C  CALCULATION FOR LOCATION OF MAXIMUM CONCRETE TEMPERATURE
76 DO 300 L=1,I
77 D1(L) = -(QV5(L)*A5(L))/(AMU5(L)*(ALPHA5(L)-1.))
78 E1(L) = AMU5(L)*(ALPHA5(L)-1.)
79 D2(L) = QV5(L)*(1.-A5(L))/(AMU5(L)*(1.+BETA5(L)))
80 E2(L) = -AMU5(L)*(1.+BETA5(L))
81 F1(L) = QV5(L)/((AMU5(L)**2)*ELX5)
82 F2(L) = A5(L)*(EXPF(E1(L)*ELX5)-1.)/((ALPHA5(L)-1.)**2)
83 F3(L) = (1.-A5(L))*(EXPF(E2(L)*ELX5)-1.)/((1.+BETA5(L))**2)
84 FTF(L) = F1(L)*(F2(L)+F3(L))
85 FT = FT +FTF(L)
86 SUM(L) = D1(L)*EXPF(E1(L)*X)+D2(L)*EXPF(E2(L)*X)
87 SUMT = SUMT + SUM(L)
88 SUMP(L) = E1(L)*D1(L)*EXPF(E1(L)*X)+E2(L)*D2(L)*EXPF(E2(L)*X)
89 SUMPT = SUMPT+SUMP(L)
300 CONTINUE
90 FX = ((T6X-T5)/ELX5)+(SUMT+FT)/CONS
91 FXP = SUMPT/CONS
92 IF(ABS(FX)-0.10) 96,96,93.
93 K3 = K3+1
94 X = X-FX/FXP
95 GO TO 73
96 CONTINUE
97 XTMAX = X
98 SMT = 0.
C  CALCULATION OF MAXIMUM CONCRETE TEMPERATURE
99 DO 400 N=1,I
101 R1(N) = QV5(N)*A5(N)/((AMU5(N)**2)*(ALPHA5(N)-1.)**2)
102 RE1(N) = (1.+EXPF(E1(N)*XTMAX))
103 R2(N) = QV5(N)*(1.-A5(N))/(AMU5(N)**2)*(1.+BETA5(N))**2)
104 RE2(N) = (1.+EXPF(E2(N)*XTMAX))
105 SMT = SMT+R1(N)*RE1(N)+R2(N)*RE2(N)+FTF(N)*XTMAX
400 CONTINUE
106 TMAX = T5+XTMAX*(T6X-T5)/ELX5+SMT/CONS
107 TMAXF = TMAX+460.
C  CALCULATION OF AIR TEMPERATURE AT TOP OF AIR CHANNEL
108 DELTOL = (QDEPT1+QDEPT2+QDEPT3+QDEPT4+QCCP+QDRAD+QCON)/(VEL*ACHAN*
1CP*3600.*RHO)
109 WRITE(51,2007)(I)
110 IF (K7-1) 1121,4999,4999
3000 WRITE(51,2000)(ELX1,ELX2,ELX3,ELX4,ELX5,T6XF,TAF)
3001 WRITE(51,2002)(QDEPT1,QDEPT2,QDEPT3,QDEPT4,QDEPT5,QCCP,QDRAD,QCON)
3002 WRITE(51,2003)(T0F,T1F,T2F,T3F,T4F,T5F)
3003 WRITE(51,2004)(DELT1,DELT2,DELT3,DELT4,DELT5,DELT6)
3004 WRITE(51,2005)(TMAXF,XTMAX,DELTOL)
109 K7 = K7+1
110 IF (K7-2) 111,5000,5000
111 TA = TA+DELTOL*HT
112 GO TO 21
1121 WRITE (51,2008)
GO TO 3000
4999 WRITE(51,2009)
GO TO 3000
3005 WRITE(51,2007)(I)
110 IF (K7-1) 4005,4006,4006
4005 WRITE(51,2008)
WRITE(51,2006)(ELX1,ELX2,ELX3,ELX4,ELX5,T6XF,TAF)
GO TO 5000
4006 WRITE(51,2009)
WRITE(51,2006)(ELX1,ELX2,ELX3,ELX4,ELX5,T6XF,TAF)
5000 CONTINUE
1000 FORMAT(8F9.0,8X)
1001 FORMAT(6F9.0,6F8.0,8X)

```

Table D.1 (continued)

2000	FORMAT(53HK) THIS CASE HAS THE FOLLOWING PHYSICAL CHARACTERISTICS , 1/// 30H LAMINATION THICKNESSES (FEET) / 8H0SKIN = ,F6.3,5X,9H INSU 2L = ,F6.3,5X,15H FIRST STEEL = ,F6.3,5X,16H SECOND STEEL = ,F6.3, 35X,12H CONCRETE = ,F6.3, /// 26H EXTERIOR CONCRETE TEMP = ,F5.1, 42X,12H (DEGREES-F), 14X,20H COOLANT AIR TEMP = ,F5.1,2X,12H (DEGREE 55-F) ///)
2002	FORMAT(66HK) GAMMA HEAT DEPOSITIONS IN EACH SEPARATE LAMINATION (BTU 1/HR-SQ FT) / 8H0SKIN = ,F9.3,2X,9H INSUL = ,F9.3,2X,15H FIRST STEEL 2 = ,F9.3,2X,16H SECOND STEEL = ,F9.3,2X,18H CONCRETE (TOT) = ,F9.3 3/24H RETURN FROM CONCRETE = ,F9.3,2X,27H RADIATION HEAT TRANSFER = 4 ,F9.3,2X,37H CONDUCTION LOSS FROM REACTOR ROOM = ,F9.3 ///)
2003	FORMAT(35HK) INTERFACE TEMPERATURES (DEGREES-F) / 21H0 REACTOR ROOM-SK 1IN = ,F9.3,15X,14H SKIN-INSUL = ,F9.3,15X,21H INSUL-FIRST STEEL = 2,F9.3 / 19H FIRST STEEL-AIR = ,F9.3,13X,20H AIR-SECOND STEEL = , 3F9.3,13X,25H SECOND STEEL-CONCRETE = ,F9.3 ///)
2004	FORMAT(52HK) TEMPERATURE DROP ACROSS EACH LAMINATION (F-DEGREES) / 19H0 T0-T1 = ,F9.4,2X, 9H T1-T2 = ,F9.4,2X,9H T2-T3 = ,F9.4,2X,9H T3 2-T4 = ,F9.4,2X,9H T4-TA = ,F9.4,2X,9H T5-T4 = ,F9.4 ///)
2005	FORMAT(32HK) MAXIMUM CONCRETE TEMPERATURE = ,F9.3,2X,12H (DEGREES-F) 1/89H DISTANCE FROM CONCRETE-STEEL INTERFACE TO LOCATION OF MAXIMUM 2 TEMPERATURE IN CONCRETE = ,F7.4,2X,7H (FEET) / 48H VERTICAL TEMPER 3ATRE GRADIENT OF COOLANT AIR = ,FR.4,2X,15H (DEGREES/FOOT))
2006	FORMAT(53H) THIS CASE HAS THE FOLLOWING PHYSICAL CHARACTERISTICS , 1/// 30H LAMINATION THICKNESSES (FEET) / 8H0SKIN = ,F6.3,5X,9H INSUL 2 = ,F6.3,5X,15H FIRST STEEL = ,F6.3,5X,16H SECOND STEEL = ,F6.3, 35X,12H CONCRETE = ,F6.3, /// 26H EXTERIOR CONCRETE TEMP = ,F5.1, 42X,12H (DEGREES-F), 14X,20H COOLANT AIR TEMP = ,F5.1,2X,12H (DEGREE 55-F) /// 93H0 THIS CASE GIVES HEAT CONDUCTION BACK INTO THE REACTO 6R ROOM AND IS THEREFORE NOT ACCEPTABLE)
2007	FORMAT(5H) (CASE, 13)
2008	FORMAT(37HK) CALCULATION AT BOTTOM OF AIR CHANNEL)
2009	FORMAT(34HK) CALCULATION AT TOP OF AIR CHANNEL)
	END

Table D.2. TSS Output Data at the Bottom of the Air Channel for One Case

CALCULATION AT BOTTOM OF AIR CHANNEL

THIS CASE HAS THE FOLLOWING PHYSICAL CHARACTERISTICS

LAMINATION THICKNESSES (FEET)

SKIN = .005 INSUL = .208 FIRST STEEL = .250 SECOND STEEL = .250 CONCRETE = 6.000

EXTERIOR CONCRETE TEMP = 50.0 (DEGREES-F) COOLANT AIR TEMP = 100.0 (DEGREES-F)

GAMMA HEAT DEPOSITIONS IN EACH SEPARATE LAMINATION (BTU/HR-SQ FT)

SKIN = 16.575 INSUL = 37.762 FIRST STEEL = 301.237 SECOND STEEL = 35.723 CONCRETE (TOT) = 36.785
 RETURN FROM CONCRETE = 27.470 RADIATION HEAT TRANSFER = 172.618 CONDUCTION LOSS FROM REACTOR ROOM = 533.620

INTERFACE TEMPERATURES (DEGREES-F)

REACTOR ROOM=SKIN = 1100.000 SKIN=INSUL = 1099.779 INSUL=FIRST STEEL = 301.936
 FIRST STEEL=AIR = 293.838 AIR=SECOND STEEL = 147.162 SECOND STEEL=CONCRETE = 147.655

TEMPERATURE DROP ACROSS EACH LAMINATION (F-DEGREES)

T0-T1 = .2213 T1-T2 = 797.8430 T2-T3 = 8.0972 T3-T4 = 195.8384 T4-TA = 47.1622 T5-T4 = .4931

MAXIMUM CONCRETE TEMPERATURE = 158.618 (DEGREES-F)

DISTANCE FROM CONCRETE-STEEL INTERFACE TO LOCATION OF MAXIMUM TEMPERATURE IN CONCRETE = .5153 (FEET)

VERTICAL TEMPERATURE GRADIENT OF COOLANT AIR = 1.5649 (DEGREES/FOOT)

Table D.3. TSS Output Data at the Top of the Air Channel for One Case

CALCULATION AT TOP OF AIR CHANNEL

THIS CASE HAS THE FOLLOWING PHYSICAL CHARACTERISTICS

LAMINATION THICKNESSES (FEET)

SKIN = .005 INSUL = .208 FIRST STEEL = .250 SECOND STEEL = .250 CONCRETE = 8.000

EXTERIOR CONCRETE TEMP = 50.0 (DEGREES-F) COOLANT AIR TEMP = 175.1 (DEGREES-F)

GAMMA HEAT DEPOSITIONS IN EACH SEPARATE LAMINATION (BTU/HR=SQ FT)

SKIN = 10,573 INSUL = 37,762 FIRST STEEL = 381,237 SECOND STEEL = 39,723 CONCRETE (TOT) = 36,705
 RETURN FROM CONCRETE = 21,989 RADIATION HEAT TRANSFER = 209,011 CONDUCTION LOSS FROM REACTOR ROOM = 486,574

INTERFACE TEMPERATURES (DEGREES-F)

REACTOR ROOM=SKIN = 1100.000 SKIN=INSUL = 1099.798 INSUL=FIRST STEEL = 367.192
 FIRST STEEL=AIR = 359.547 AIR=SECOND STEEL = 228.462 SECOND STEEL=CONCRETE = 228.902

TEMPERATURE DROP ACROSS EACH LAMINATION (F=DEGREES)

T0-T1 = .2022 T1-T2 = 732.6061 T2-T3 = 7.6449 T3-T4 = 184.4293 T4-TA = 53.3445 T5-T4 = .4404

MAXIMUM CONCRETE TEMPERATURE = 235.493 (DEGREES-F)

DISTANCE FROM CONCRETE-STEEL INTERFACE TO LOCATION OF MAXIMUM TEMPERATURE IN CONCRETE = .3568 (FEET)

VERTICAL TEMPERATURE GRADIENT OF COOLANT AIR = 1.5440 (DEGREES/FOOT)

Appendix E

NOMENCLATURE

- A = dimensionless constant used in the Taylor buildup equation
 A_1 = unit area of reactor room wall, ft^2
 C_P = specific heat at constant pressure, $\text{Btu}/\text{lb}\cdot^\circ\text{F}$
 E = energy of incident gamma current, Mev
 H = vertical length of air channel, ft
 h = convective heat transfer coefficient, $\text{Btu}/\text{hr}\cdot\text{ft}^2\cdot^\circ\text{F}$
 k = thermal conductivity, $\text{Btu}/\text{hr}\cdot\text{ft}\cdot^\circ\text{F}$
 \bar{k}_{a-b} = equivalent conductivity where the subscripts a and b refer to any two adjacent materials
 L = thickness of a material lamination
 L_{ch} = width of air channel (distance between adjacent surfaces of first and second steel gamma shields), ft
 MWL = heat conduction rate out of the reactor room to the air channel, Mw
 Q = volumetric gamma heating rate, $\text{Btu}/\text{hr}\cdot\text{ft}^3$
 q^* = heat conduction rate out of the reactor room to the air channel, $\text{Btu}/\text{hr}\cdot\text{ft}^2$
 q'_c = rate at which the gamma heat generated in the concrete is conducted back toward the air channel, $\text{Btu}/\text{hr}\cdot\text{ft}^2$
 q_R = rate of radiant heat transfer between the walls of the air channel, $\text{Btu}/\text{hr}\cdot\text{ft}^2$
 T = temperature, $^\circ\text{F}$
 U_a = bulk velocity of coolant air, ft/sec
 x = distance perpendicular to the surface of the reactor room wall, ft
 α and β = dimensionless constants used in the Taylor buildup equation
 ϵ = surface emissivity of walls of air channel
 θ = time, hours
 μ = total gamma attenuation coefficient, ft^{-1}
 μ_E = gamma energy attenuation coefficient, ft^{-1}

- ρ = density, lb/ft³
 σ = Stefan-Boltzmann constant
 Φ_0 = incident gamma current, photons/cm²·sec

Subscripts Used With Terms

- 0 through 6 = numbers denoting a lamination interface as illustrated
in Fig. 2 and usually associated with temperature, T
- a = air
c = concrete
I = insulation
i = energy group
j = lamination
s = skin lamination on reactor side of wall
FS = first steel gamma shield
SS = second steel gamma field
T = total

.C.

RECEIVED

.C.

Internal Distribution

- | | |
|-----------------------|--------------------------------------|
| 1. M. Bender | 26. R. L. Moore |
| 2. C. E. Bettis | 27. H. A. Nelms |
| 3. E. S. Bettis | 28. E. L. Nicholson |
| 4. E. G. Bohlmann | 29. L. C. Oakes |
| 5. R. B. Briggs | 30. A. M. Perry |
| 6-7. W. K. Crowley | 31. T. W. Pickel |
| 8. F. L. Culler | 32-33. J. R. Rose |
| 9. S. J. Ditto | 34-35. M. W. Rosenthal |
| 10. H. G. Duggan | 36. Dunlap Scott |
| 11. D. A. Dyslin | 37. W. C. Stoddart |
| 12. D. E. Ferguson | 38. D. A. Sunberg |
| 13. W. F. Ferguson | 39. R. E. Thoma |
| 14. F. C. Fitzpatrick | 40. H. K. Walker |
| 15. C. H. Gabbard | 41. J. R. Weir |
| 16. W. R. Gall | 42. M. E. Whatley |
| 17. W. R. Grimes | 43. J. C. White |
| 18. A. G. Grindell | 44. W. R. Winsbro |
| 19. P. N. Haubenreich | 45-46. Central Research Library |
| 20. H. W. Hoffman | 47. Document Reference Section |
| 21. P. R. Kasten | 48. GE Division Library |
| 22. R. J. Kedl | 49-58. Laboratory Records Department |
| 23. G. H. Llewellyn | 59. Laboratory Records, ORNL R. C. |
| 24. R. E. MacPherson | 60. ORNL Patent Office |
| 25. H. E. McCoy | |

External Distribution

61. P. F. Pasqua, Nuclear Engineering Department, University of Tennessee, Knoxville, Tennessee
62. L. R. Shobe, Engineering Mechanics Department, University of Tennessee, Knoxville, Tennessee
- 63-77. Division of Technical Information Extension
78. Laboratory and University Division, USAEC, ORO